

# UC San Diego

## Research Theses and Dissertations

### Title

Lessons from Nature: Novel Routes to Biomimetic Synthesis of Silica Based Materials

### Permalink

<https://escholarship.org/uc/item/0xb2350z>

### Author

Cha, Jennifer N.

### Publication Date

2000-12-01

Peer reviewed

## **INFORMATION TO USERS**

**This manuscript has been reproduced from the microfilm master. UMI films the text directly from the original or copy submitted. Thus, some thesis and dissertation copies are in typewriter face, while others may be from any type of computer printer.**

**The quality of this reproduction is dependent upon the quality of the copy submitted. Broken or indistinct print, colored or poor quality illustrations and photographs, print bleedthrough, substandard margins, and improper alignment can adversely affect reproduction.**

**In the unlikely event that the author did not send UMI a complete manuscript and there are missing pages, these will be noted. Also, if unauthorized copyright material had to be removed, a note will indicate the deletion.**

**Oversize materials (e.g., maps, drawings, charts) are reproduced by sectioning the original, beginning at the upper left-hand corner and continuing from left to right in equal sections with small overlaps.**

**Photographs included in the original manuscript have been reproduced xerographically in this copy. Higher quality 6" x 9" black and white photographic prints are available for any photographs or illustrations appearing in this copy for an additional charge. Contact UMI directly to order.**

**ProQuest Information and Learning  
300 North Zeeb Road, Ann Arbor, MI 48106-1346 USA  
800-521-0600**

**UMI<sup>®</sup>**



**UNIVERSITY OF CALIFORNIA**  
**Santa Barbara**

**Lessons from Nature: Novel Routes to Biomimetic  
Synthesis of Silica based Materials**

**A Dissertation submitted in partial satisfaction  
of the requirements for the degree of**

**Doctor of Philosophy**

**in**

**Inorganic Chemistry**

**by**

**Jennifer Nam Cha**

**Committee in charge:**

**Professor Galen D. Stucky, Chairperson**  
**Professor Daniel E. Morse**  
**Professor Timothy J. Deming**  
**Professor Fred F. Lange**

**December 2000**

UMI Number: 3020262

**UMI<sup>®</sup>**

---

**UMI Microform 3020262**

**Copyright 2001 by Bell & Howell Information and Learning Company.**

**All rights reserved. This microform edition is protected against  
unauthorized copying under Title 17, United States Code.**

---

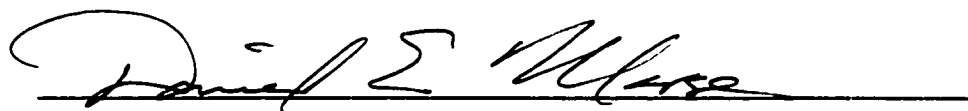
**Bell & Howell Information and Learning Company**

**300 North Zeeb Road**

**P.O. Box 1346**

**Ann Arbor, MI 48106-1346**

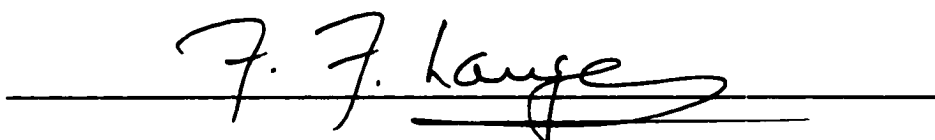
This dissertation of Jennifer N. Cha is approved

A handwritten signature in cursive script, reading "Daniel E. Morse", positioned above a solid horizontal line.

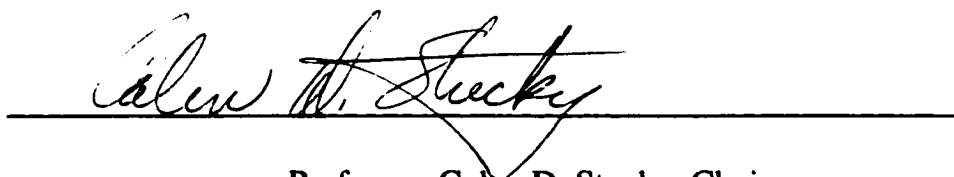
Professor, Daniel E. Morse

A handwritten signature in cursive script, reading "Timothy J. Deming", positioned above a solid horizontal line.

Professor, Timothy J. Deming

A handwritten signature in cursive script, reading "Fred F. Lange", positioned above a solid horizontal line.

Professor, Fred F. Lange

A handwritten signature in cursive script, reading "Galen D. Stucky", positioned above a solid horizontal line.

Professor, Galen D. Stucky, Chairperson

**December 12, 2000**

**Copyright by  
Jennifer N. Cha**

**2000**

## ACKNOWLEDGMENTS

It is difficult to acknowledge a thesis because it often is a work that is a culmination of a significant part of one's lifespan and experiences both inside and outside of the lab contribute greatly to it.

I would foremost like to thank my advisors, Professor Dan Morse and Professor Galen Stucky for their incredible support towards my research as scientists, thesis advisors and mentors. They have entrusted me numerous times throughout the past four years to pursue areas that I thought would be worthwhile to look into and they have encouraged me to be both creative and thorough. For all these reasons, I thank them both very much.

I would also like to thank Professor Tim Deming for allowing me to do research in his lab in the latter two years and for his patience and all of his excellent scientific advice.

Being part of a multidisciplinary group, there are not surprisingly many students and postdoctoral researchers I would like to acknowledge for both their research expertise and their friendship. I would like foremost to thank the postdoctoral researchers, Dr. Katsuhiko Shimizu and Dr. Yan Zhou for all of their help with the molecular biology and protein chemistry. I would also like to give my warmest thanks to James Weaver for his expert help in invertebrate



biology and most of all for his telling me of the perfect biosilicate to study. I would also like to give my warmest thanks to Neal Hooker and Bonnie Bosma for all of their help in extracting the proteins the proteins as well as for helping me with any mishaps I caused in the lab (there weren't too many I hope....) I would also to thank Dr. Giuseppe Falini for giving me my first lessons in biomineralization and for giving great pizza parties.

Another person who deserves many thanks is Dottie McLaren for all of her fantastic help with the figures for group meetings, posters, conference talks and for this thesis.

Sean Christiansen deserves many thanks for his help in the silicon NMR of all of my samples. I have never known a person to be so patient and understanding and he has always been there ready to answer all of my questions and help out whenever necessary. I would also like to thank Michael Mann for his NMR advice as well as for his friendship.

I would like to give a thanks to Scott Curtin and Joon Hwang for answering all of my technical questions and to Mike Wyrsta for making me laugh, exchanging ideas and for trying to share a lab bench with me--sometimes. I also want to thank him for the numerous times he's given me some of his NCAs and his initiators.

Although I didn't do much of my Ph.D. work in Galen's lab, I would like

to thank Brian Scott for helping me get set up the last few months in the lab and for answering all of my questions and teaching me quite a bit about optical based materials. (Brian, try to come back alive after you've run down the Grand Canyon and come up the other side in October).

Finally, I would like to give my especial thanks and love to Erik for being my best friend and for sharing his life with me.

## VITA

Born December 4, 1971

San Francisco, CA

## EDUCATION

September, 1989 – June, 1991

University of CA, Davis, 3.7 GPA

June, 1991- December, 1993

University of CA, Berkeley, B.A. received  
in Developmental Cell Biology

March, 1995- present

University of CA, Santa Barbara,  
Department of Chemistry, 3.8 GPA  
Ph.D. awarded December, 2000

## RESEARCH AND TEACHING EXPERIENCE

September, 1990- June, 1991

assistant researcher, Cancer Research  
Center, UC Davis Medical Center

September, 1991- June, 1994

assistant researcher, tissue culture facility,  
UC Berkeley

June, 1995- September, 2000

Graduate student researcher,  
Department of Chemistry, UC Santa  
Barbara

March, 1995- June, 1996

Teaching assistant, inorganic and organic  
chemistry laboratories, UC Santa Barbara

June, 1996- September, 1999

Research mentor for high school and UCSB  
undergraduate students (QUEST and MRL  
programs)

## PUBLICATIONS

1. K.Shimizu, J.N. Cha, G.D. Stucky, D.E. Morse, "Silicatein  $\alpha$ : Cathepsin L-like protein in sponge biosilica", *Proc. Nat. Acad. Sci.*, **95**, 6234-6238 (1998)
2. J.N. Cha, K. Shimizu, Y. Zhou, S.C. Christiansen, B.F. Chmelka, G.D. Stucky, D.E. Morse, "Silicatein filaments and subunits from a marine sponge direct the Polymerization of silica and silicones *in vitro*", *Proc. Nat. Acad. Sci.*, **96**, 361-365 (1999)
3. Y. Zhou, K. Shimizu, J.N. Cha, G.D. Stucky, D.E. Morse, "Efficient catalysis of polysiloxane synthesis by silicatein  $\alpha$  requires specific hydroxyl and imidazole functionalities", *Angew. Chem. Int. Ed.*, **38**, 780-782 (1999)
4. J.N. Cha, G.D. Stucky, D.E. Morse, T.J. Deming, "Block Copolypeptide Mediated Biomimetic Synthesis of Ordered Silica Structures", *Nature*, **403**, 289-292 (2000)
5. J. N. Cha, K. Shimizu, Y. Zhou, T.J. Deming, G.D. Stucky, D.E.Morse "Learning from Nature: Novel Routes to Biomimetic Synthesis of Silica Structures", *MRS Symposium (Mineralization in Natural and Synthetic Biomaterials, Boston, November, 1999)*
6. J.N. Cha, T.J.Deming, D.E. Morse, G.D. Stucky, "Ordered Syntheses of Silica and Silsequioxanes via Interfacial Catalysis", *ACS Symposium, Solid State Inorganic Chemistry, San Francisco, March, 2000*

Some of thesis work also discussed in:

D.E. Morse, "Silicon biotechnology: proteins, genes and molecular mechanisms controlling biosilica nanofabrication offer new routes to polysiloxane synthesis", *Organosilicon Chemistry IV: from Molecules to Materials* (Eds. N. Auner & J. Weis) (Wiley-VCH, New York, in press)

## PATENTS

- 1.) "Silica, Polysilsequioxane, Polysiloxane and Polymetallo-oxane Syntheses", D.E. Morse, G.D.Stucky, T.J.Deming, J.N. Cha, K. Shimizu, Y.Zhou, December, 1998
- 2.) "Using the bioluminescence from single strands of DNA to build a variety of sensors ranging from DNA detection to gene chip arrays to DNA based optical devices", J.N.Cha, B. Scott, G.D. Stucky, D.E. Morse, July, 2000

## ATTENDED CONFERENCES

1. Poster, 1997,1998,1999: "MURI Workshop", University of CA, Santa Barbara, CA
2. Talk, October 31, 1999: "Composites at Lake Louise, 1999", Lake Louise, Canada
3. Talk, November 30, 1999: "Materials Research Society, 1999", Boston, MA
4. Talk, March 28, 2000: "American Chemical Society, 2000", San Francisco, CA
5. Poster, April 3, 2000: "International Workshop on Advances in Materials Science and Technology", Singapore
6. Talk, June 5, 2000: Conference. "Society for Experimental Mechanics, Inc.", Orlando, FL, *invited*
7. Talk, August 15, 2000: "Gordon Research Conference, Biomineralization", New Hampshire, *invited*
8. Talk, December 16, 2000: "American Chemical Society, 2000", Honolulu, HI, *invited*

## **HONORS**

- 1. Golden Key National Honor Society, University of CA, Davis**
- 2. California Sea Grant Trainee, June, 1996- present**
- 3. Materials Research Travel Fellowship, July, 2000**

**If you can't convince them, confuse them.**  
*Harry S. Truman*

## ABSTRACT

### Lessons from Nature: Novel Routes to Biomimetic Synthesis of Silica Based Materials

by

Jennifer N. Cha

In nature, biominerals are formed under the control of organic components such as proteins and polysaccharides at ambient pHs and temperatures. Yet up until recently, there has been little success in utilizing such constituents as templates for biomimetic silica synthesis. Our recent studies here at UCSB of the proteins occluded within silica needles of the sponge, *Tethya aurantia*, demonstrate that the proteins which we've named silicateins (silica proteins), have the capability of acting as catalysts for the hydrolysis of silicon alkoxides at physiological pH and temperature, while also serving as scaffolds to organize the resulting silica or silisequioxane products. It is well understood among silica chemists that silicon alkoxides normally must undergo acid or base hydrolysis prior to condensation to silicon dioxide and is therefore normally very stable at pH 7. The understanding of the mechanism of these silicateins arose from mutagenesis studies of the proteins and it was from these results that block copolypeptides were designed. These polymers could not only accelerate the polycondensation of silica from silicon alkoxides at neutral pH but also contained self assembling features, either through hydrogen, ionic or covalent bonding. It was discovered that the utilization of these varying polypeptides allowed us to successfully synthesize ordered silica structures ranging from transparent silica spheres to bundles of lathlike silica structures at ambient temperature, pressure and pH.



## TABLE OF CONTENTS

<b>I. Background</b>	
A. Introduction	pp. 1-2
B. The Organic Matrix	pp. 3-12
C. Silicification in Microenvironments: the Cell and the Silicon Deposition Vesicle	pp. 13-14
D. The Elusive Species used for Biosilicification	pp. 15-16
E. Biomimetic Synthesis of Silica	pp. 17-18
<b>II. Chapter 1: The Organic Matrix of the Sponge Spicules</b>	pp. 22-37
<b>III. Chapter 2: Activity of the Biological Proteins</b>	pp. 38-48
<b>IV. Chapter 3: The Template</b>	pp. 49-65
<b>V. Chapter 4: Learning from Nature: Routes to Biomimetic Silica Synthesis</b>	pp. 66-87
<b>VI. Chapter 5: Block Copolypeptide Design for Biomimetic Silica Synthesis</b>	pp. 88-106

## LIST OF FIGURES

Figure 1: Scanning electron images of cleaned diatom frusutles	p. 2
Figure 2: Hecky <i>et al</i> 's hypothetical scheme	p. 4
Figure 3: Lobel's computational modeling scheme	p. 6
Figure 4: The chemical structure of the silaffins	p. 7
Figure 5: Silica product from reacting the silaffins with silicic acid	p. 8
Figure 6: Venus' basket sponge	p. 9
Figure 7: SEM image of a fractured spicule	p. 10
Figure 8: Cross section of a spicule (courtesy of James Weaver and Prof. Dan Morse)	p. 12
Figure 9: A schematic diagram of silicon transport into a diatom cell (courtesy of Mark Hildebrand, <i>Scripps</i> )	p. 14
Figure 10: <i>Tethya aurantia</i> or the "Orange Puffball Sponge"	p.23
Figure 11: Light and scanning electron images of the spicules extracted from the <i>Tethya aurantia</i>	p. 24
Figure 12: An image of a bifurcated spicule from <i>Tethya aurantia</i>	p. 25
Figure 13: A SEM image of a partially etched spicule	p. 27
Figure 14: A SEM image of the silicatein (axial) filaments	p. 28
Figure 15: Small angle x-ray data of the silicateins air-dried on glass coverslips	p. 29
Figure 16: A SDS-PAGE of the silicatein filaments	p. 30
Figure 17: The amino acid sequence of silicatein $\alpha$	p. 33

<b>Figure 18: Comparison of silicatein <math>\alpha</math>'s sequence with that of human cathepsin L</b>	<b>p. 34</b>
<b>Figure 19: The catalytic triad of serine proteases</b>	<b>p. 35</b>
<b>Figure 20: Hydrophilicity/phobicity plots for both silicatein <math>\alpha</math> and human cathepsin L</b>	<b>p. 39</b>
<b>Figure 21: A model of silicatein <math>\alpha</math></b>	<b>p. 40</b>
<b>Figure 22: The general reaction scheme of silicon alkoxides</b>	<b>p. 42</b>
<b>Figure 23: SEM images of the silicatein filament before and after reaction with TEOS at pH 7</b>	<b>p. 51</b>
<b>Figure 24: A SEM image of air-dried silicatein filaments after reaction with neat TEOS (no water in the reaction mixture except that for protein hydration)</b>	<b>p. 52</b>
<b>Figure 25: SEM images of cellulose fibers before and after reaction with TEOS at pH 7</b>	<b>p. 53</b>
<b>Figure 26: <math>^{29}\text{Si}</math> MAS NMR analyses of the silicatein filaments after reaction with TEOS</b>	<b>p. 54</b>
<b>Figure 27: A SEM image of the silicatein filaments after reaction with phenyltriethoxysilane at pH 7</b>	<b>p. 56</b>
<b>Figure 28: Cross polarization <math>^{29}\text{Si}</math> MAS NMR results of the silicatein filaments after reaction with phenyltriethoxysilane at pH 7</b>	<b>p. 57</b>
<b>Figure 29: A proposed mechanism of silicon alkoxide hydrolysis by the silicateins</b>	<b>p. 60</b>
<b>Figure 30: The silicateins' catalytic activity after site-directed mutagenesis</b>	<b>p. 63</b>
<b>Figure 31: A schematic diagram of functional groups at the organic inorganic interface which could hydrolyze silicon alkoxides such as TEOS.</b>	<b>p. 68</b>
<b>Figure 32: The reaction scheme of BpyNiCOD and NCAs</b>	<b>p. 70</b>

<b>Figure 33: NCA synthesis by phosgene</b>	<b>p. 71</b>
<b>Figure 34: The protected L-amino acids used to make the various polypeptides</b>	<b>pp.72-74</b>
<b>Figure 35: SEM images of lyophilized samples of a random and a block copolypeptide</b>	<b>p. 76</b>
<b>Figure 36: Summary of hypothetical design on how to biomimetically create ordered silica structures</b>	<b>p. 77</b>
<b>Figure 37: SEM image of silica product formed after reaction poly-L-proline and TEOS at pH 7</b>	<b>p. 83</b>
<b>Figure 38: Examples of amino acids that could be incorporated to form diblock copolypeptides that would self-assemble</b>	<b>pp.89, 90</b>
<b>Figure 39: The chemical structures of the various diblock copolypeptides that were synthesized for biomimetic silica synthesis</b>	<b>pp.93, 94</b>
<b>Figure 40: SEM images of the silica structures that were formed after reacting some of the diblock copolypeptides with TEOS at pH 7</b>	<b>p. 98</b>
<b>Figure 41: Light and scanning electron images of the silica formed after reacting both the reduced and oxidized form of poly(L-cysteine<sub>30</sub>-L-lysine<sub>200</sub>) with TEOS at pH 7</b>	<b>p. 100</b>
<b>Figure 42: A hypothetical scheme of how silica synthesis may occur in the emulsified reaction between the block copolypeptides and TEOS</b>	<b>p. 102</b>

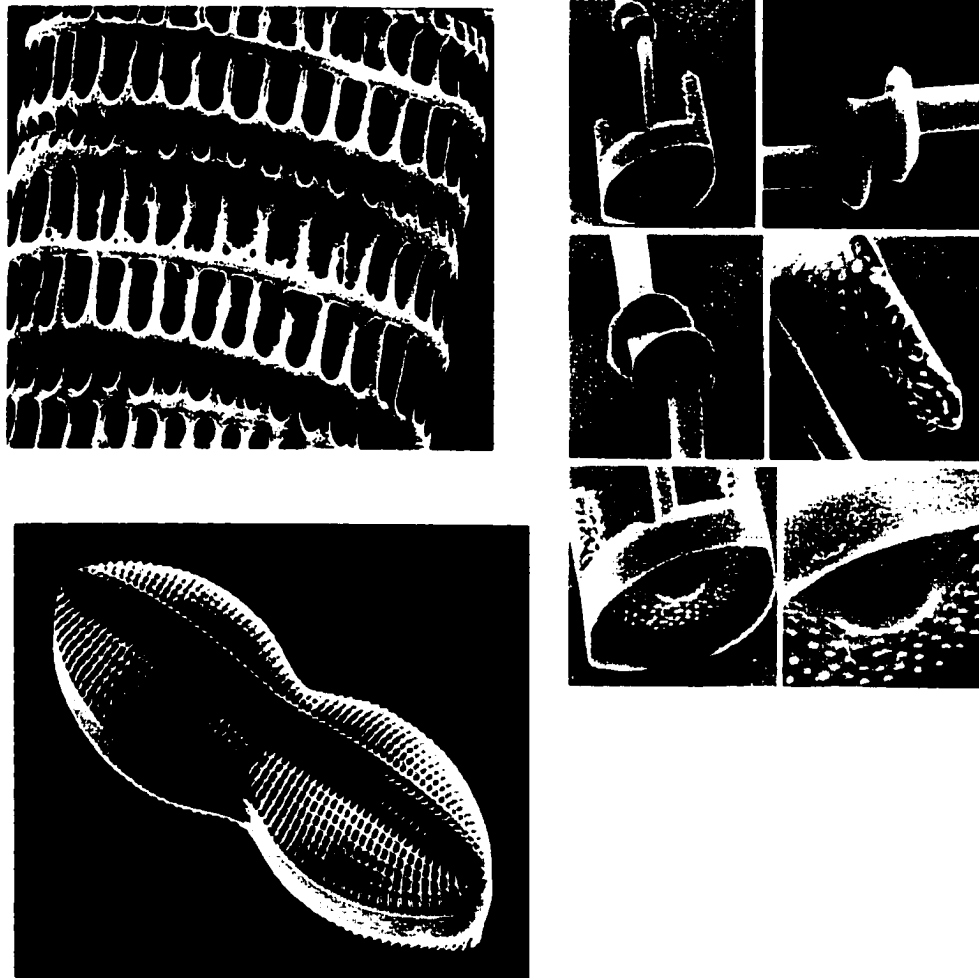
## LIST OF TABLES

Table 1. Net difference in amino acid composition between the diatoms' cell walls and cellular contents ( <i>reproduced from Hecky et al., Marine Biology, 1973</i> )	p. 4
Table 2. Hecky's amino acid analyses of sponge spicules	p. 11
Table 3. Silica and the occluded protein yield from <i>Tethya aurantia</i>	p. 26
Table 4. Amino acid composition of the intact silicatein(axial) filaments and of each of the silicatein subunits ( $\alpha$ , $\beta$ , and $\gamma$ )	p. 31
Table 5. The amount of silica produced from reacting various proteins with TEOS at pH 7	p. 45
Table 6. Amounts of silica produced from reacting various polypeptides with TEOS at pH 7	p.81
Table 7. Amounts of silica produced from reacting different combinations of polypeptides with TEOS at neutral pH	p.85
Table 8. Amounts of silica produced from reacting various block copolypeptides with TEOS at pH 7.	p. 96

## **A. Introduction**

Research into the mechanisms that control biomineralization of either crystalline or amorphous materials have demonstrated the importance of the organic matrices as structure directing templates(1-6). In both the calcium carbonate ( $\text{CaCO}_3$ ) and silica ( $\text{SiO}_2$ ) systems, proteins and proteoglycans have been targeted as the key organic components.

In many life forms, silicon is considered to be an essential element, for both structural and metabolic aspects (7). One class of unicellular plants, the diatoms, utilize silica to produce beautiful and intricate cell walls, termed frustules (Figure 1). As one can easily see from the scanning electron micrographs shown below, diatoms have the unique capability of producing a wide variety of silica shapes with a nanoscale precision that is currently difficult to duplicate in laboratories.



**Figure 1.** Scanning electron images of cleaned diatom frustules from a variety of different species

## B. The Organic Matrix

As is demonstrated in the previous SEM images, diatoms have the capability of creating ordered infrastructures of amorphous silicon dioxide in physiological conditions. From Hecky *et al's* analysis of the amino acids extracted from diatom frustules, the organic template responsible for organizing the silica was thought to be amino acid based (8). By comparing to the intracellular amino acids of 6 diatom species, Hecky discovered that a higher percentage of hydroxylated amino acids such as L-serine (Table 1) were occluded within the siliceous frustule. In the experiments listed, the diatoms were first resuspended in triple distilled water and sonicated in order to remove the cellular contents. The cell walls were then collected by centrifugation and the silica was dissolved away by HF. Amino acid analyses were then done by acid hydrolysis on the soluble contents after HF dissolution. Table 1 shows the net percentage differences between the cells walls (**a**) and the cellular contents (**b**).



Amino acids	<i>Navicula pelliculosa brevis</i>	<i>Melosira granulata</i>	<i>Cyclotella stelligera</i>	<i>Cyclotella cryptica</i>	<i>Nitzschia</i>
Serine + threonine	+15	+136	+170	+178	+31
Glycine	+15	+36	+85	+98	+5
Glutamic acid+ aspartic acid	-54	-54	-66	-47	-46
Tyrosine + phenylalanine	-3	-36	-67	-50	-7
Methionine + cysteine	-8	-5	-20	-26	-29

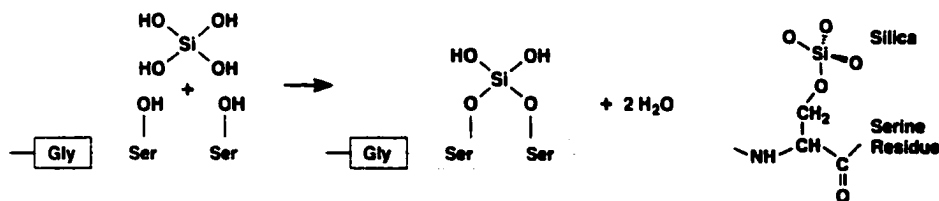
Numbers shown are net percentage differences between cell-wall compositions and cell contents for the amino acids shown (a - b) (reproduced from Hecky et al., *Mar. Biol.*, **19**, 323-331)

**Table 1.** Net differences in amino acid composition between the cell walls and the cellular contents

The results obtained by Hecky suggested that hydroxylated amino acids such as serine and threonine could organize silica by undergoing condensation reactions with silicic acid, thereby "epitaxially" growing silica directly from the protein

**Proposed Condensation Reaction:**

R. E. Hecky et al., *Marine Biology* 19 (1973) pp. 323-331



template (Figure 2).

**Figure 2.** Hecky et al's hypothetical scheme of silicification at the organic matrix

Although no actual proteins were extracted and no exact sequences were determined, Hecky's hypothetical scheme was that a string of hydroxylated amino acids such as L-serine would first hydrogen bond with mono- or orthosilicic acid followed by a condensation reaction to form covalent C-O-Si linkages; this initial layer would then promote condensation with other silicic acid molecules.

Hecky's amino acid analyses of the uncleaned diatom frustules were supported in part by the research of Swift and Wheeler (9). While the previous data presented was on the amino acid contents of the entire cell wall, Swift and Wheeler analyzed the amino acids specifically occluded within the silica of the diatom cell wall. They did this by first treating the sonicated diatom cell walls with sodium hypochlorite (NaOCl) in order to remove the organic casing of the frustules. The cleaned cell walls were then further treated with a 1M: 5M HF: NH<sub>4</sub>F in order to dissolve the silica. Their studies of the amino acid contents occluded within the silica did not differ greatly from that of Hecky's.

The hypothetical scheme shown in Figure 2 was supported further by computational studies done by Lobel *et al* (10,11). For the computational modeling, it was assumed that the organic matrix adopts a  $\beta$ -sheet secondary structure and this was based on the fact that the amino acid compositions found were similar to that of  $\beta$ -sheet forming keratin. The sequence of the template was hypothetical in nature but the calculations from a 24-stage reaction pathway gave an activation barrier of +15.4 kcal mol<sup>-1</sup> and a net stabilization of -28 kcal mol<sup>-1</sup> for the final formation of the tetrasiloxane rings shown in Figure 3. The course of

the reaction was the initial condensation of two silicic acid molecules to adjacent serines to the condensation between the two silicic acids to give disilicic acid which then condensed further with orthosilicic silicic acid molecules to form the tetrasiloxane rings.

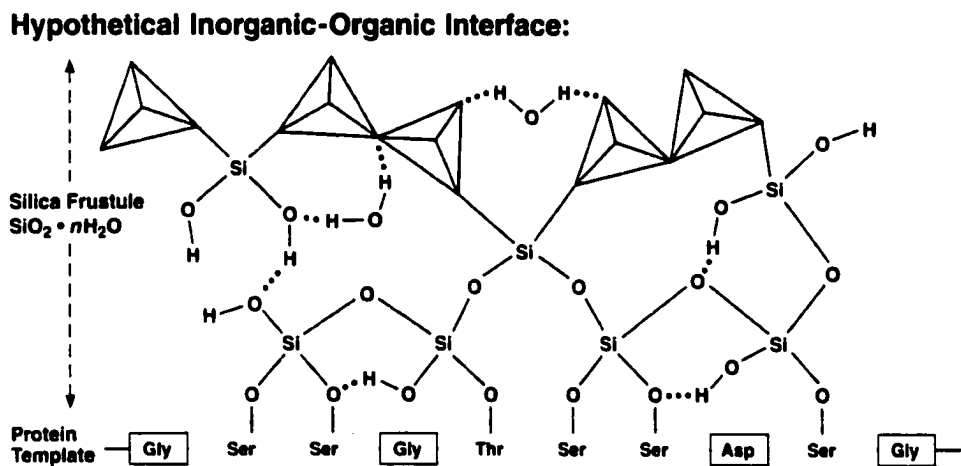


**Figure 3.** Lobel's computational modeling scheme (from Lobel et al., *Marine Biology*, 126, 353-360)

In the recent years, an enormous effort on the part of Nils Kröger and Manfred Stump has revealed much of the nature of the organic material associated with diatom frustules. They have both sequenced and characterized a number of proteins from the silicified walls of diatoms (*Cylindrotheca fusiformis* and *Navicula pelliculosa*), including those they have named frustulins, HEPs (HF-extractable proteins) and

silaffins (4-6, 12). The frustulins are a highly conserved family of glycoproteins composed of repetitive amino acid sequence motifs and calcium binding sites. Immunohistochemical studies were performed and they suggested that the frustulins are not directly associated with the silica but with the casing of the frustule which has been thought to prevent silica dissolution from occurring. On the other hand, HEPs and silaffins were extracted as the occluded organic material within the diatom frustule.

The silaffins are a family of occluded, polycationic peptides and are particularly rich in the basic amino acids, lysine and arginine (12). The clusters of lysine and arginine are regularly spaced with the hydroxyl residues, primarily serine and tyrosine. One of the most unique characteristics of the silaffins is the post-translational modifications of the lysine to  $\epsilon$ -N,N-dimethyllysine and oligo-N-methyl-propylamine, increasing the overall positive charge of the peptides at neutral pH. (Figure 4).

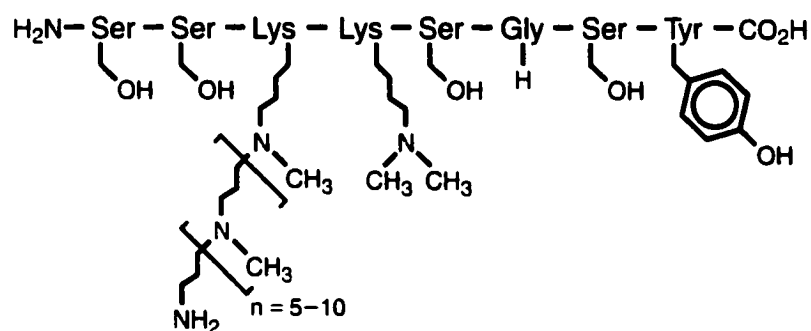
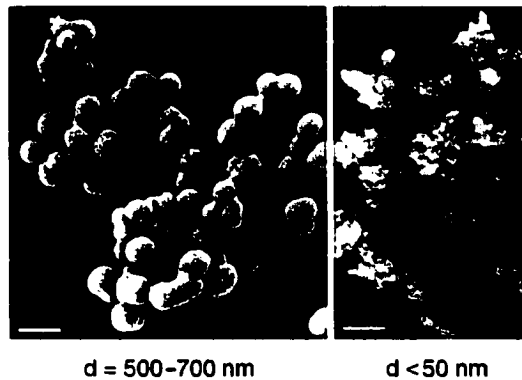


**Figure 4.** The chemical structure of the silaffins [Kroeger *et al.*, *Science*, **286**, 1129 (1999)]

In their *in vitro* studies, the silaffins have been demonstrated to both accelerate the polycondensation of stable silicic acid species at pH 5 and to also direct the polymerization to form nano-spheres (Figure 5).



Kröger et al.  
*Science* **286**: 1129 (1999)

**Figure 5.** Silica product from reacting the silaffins with monosilicic acid

Interestingly enough, such nanospheres have been observed in the substructure of cleaned diatom frustules and many hypotheses on how these spheres would form had been postulated. It was not until Kröger's recent discoveries that any clear scientific evidence has been put forth.

Aside from the diatoms, sponges are a class of animals that utilize silica to form their endoskeletons; the individual glassy needles are termed spicules. In order to form the skeletal framework, the spicules can be fused or interlocking as is shown in the beautiful photograph of the sponge, Venus' basket sponge, shown in Figure 6.

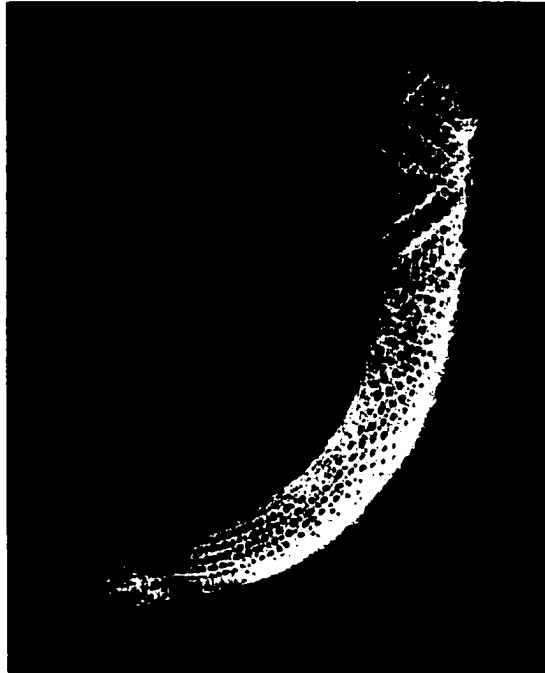


**Figure 6.** The silica endoskeleton of the sponge, Venus' basket sponge.

It has been known for some time that within each spicule exists an organic core called the axial filament that can be isolated by dissolving the silica away with hydrofluoric acid. An axial filament is shown in this SEM image of a fractured spicule as the triangular shaped fiber running down the center of the glassy matrix (Figure 7)

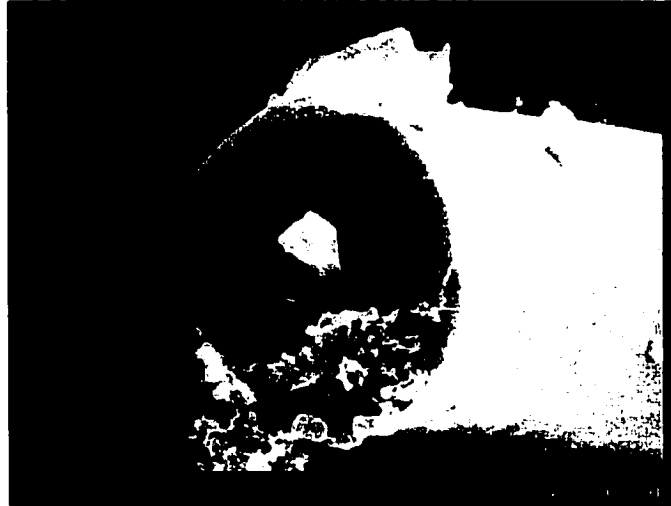


**Figure 7.** An SEM image of a fractured spicule showing the axial filament in the center

As early as 1901, it was discovered by Büschli that proteins existed in the axial filaments (13). Amino acid analyses of the axial filaments were also done by Hecky and the different amino acid distributions between the spicules and the sponge tissue is shown in Table 2 (8). These results are very similar to Hecky's other amino acid analyses of the diatom frustules, indicating that the process of silicification between the diatoms and sponges may be similar in nature.

### **Siliceous sponge spicules**

<b>Amino acids</b>	<b>Difference between Spicule &amp; Sponge Tissue</b>
Serine + Threonine	+15
Glutamic acid + aspartic acid	-28
Glycine	+35
Tyrosine + phenylalanine	-43
Methonine + cysteine	-12

*reproduced from Hecky et al., Mar. Biol. (1973)*

**Table 2.** Hecky's amino acid analysis of sponge spicules

The idea that the axial filaments may act as direct templates for silicification was suggested when researchers extracted branched axial filaments from branched spicules, implying that the final morphology of the spicule directly follows that of the organic filaments.

Schwab and Shore also discovered that when broken spicules were etched in HF and analyzed by both electron microscopy and carbon replicas, extensive ring structures were observed in the silica (14). Furthermore, they found that the rings disappeared when the spicules were calcined, indicating that the rings were formed from either thin organic layers or water. These ring structures were also observed at UCSB in SEM images of fractured *Tethya aurantia* spicules (Figure 8).



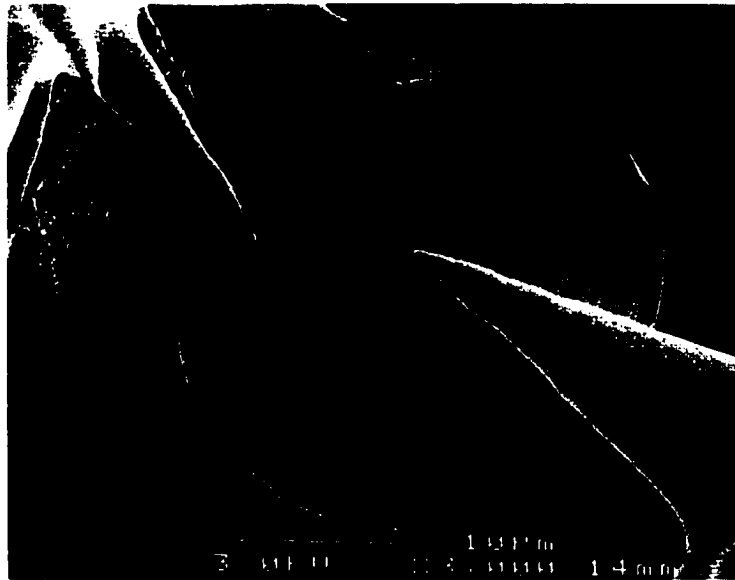


**Figure 8.** Cross section of a spicule from *Tethya aurantia*  
(courtesy of James Weaver and Prof. Dan Morse, UCSB)

These structures suggest that organic constituents apart from the axial filaments may also assist in the process of silicification.

Higher plants such as the *Equisetum arvense* (Common horsetail) have also been studied extensively by Perry (Harrison) *et al* and here, an occluded organic matrix was found to contain both protein and carbohydrates, namely xylose and glucose (15, 16). In general, two sets of soluble organic materials have been isolated, one rich in hydroxyl and glycine residues and the other in lysine and proline. A third insoluble material has been characterized as having up to 26 mole% lysine and a high level of proline and aliphatic amino acids.

### C. Silicification in Microenvironments: the Cell and the Silicon Deposition Vesicle (SDV)

Aside from the amino acid compositions, another common feature among biosilicates is the membrane bound organelle termed the silicon deposition vesicle or SDV--the nanoscale environment in which biosilicification occurs. Transmission electron images have shown that the SDV play a distinct role in directing the final shape of the silica. Because of the difficulty in deciphering the pH of the SDV, it is not yet known at whether silicification occurs at acidic, neutral or basic pH. Recently, some studies using pH sensors have shown the pH of the SDV to be acidic in nature but this remains disputable (17).

In 1996, Hildebrand *et al* discovered a family of genes that coded for a set of membrane proteins, appropriately termed silicon transporters (18) since they proved to be responsible for delivering silicic acid into the diatom from the exterior sea or freshwater environment. This mechanism of silica transport was proven when Hildebrand injected the messenger RNA (mRNA) of the silicon transporter genes into living frog eggs. Although these frog oocytes were previously unable to uptake silicic acid into their cells, upon the expression of the silicon transporter genes, the frog cells acquired the ability to do so. The three dimensional structure of the protein sequences demonstrated that the silicon transporters are composed of 12 helical transmembrane domains and are thought to form a cylindrical barrel across the lipid bilayer of the cell membrane. Although

there is no concrete data as of yet, there still remains the possibility that some silicon transporters exist in the outer cell membrane of the diatom cell while others may exist in the membrane of the SDV. Figure 9 depicts the scheme of silicon transport that may occur in the diatoms (*courtesy of Dr. Mark Hildebrand and Prof. Ben Volcani, Scripps Institute*).

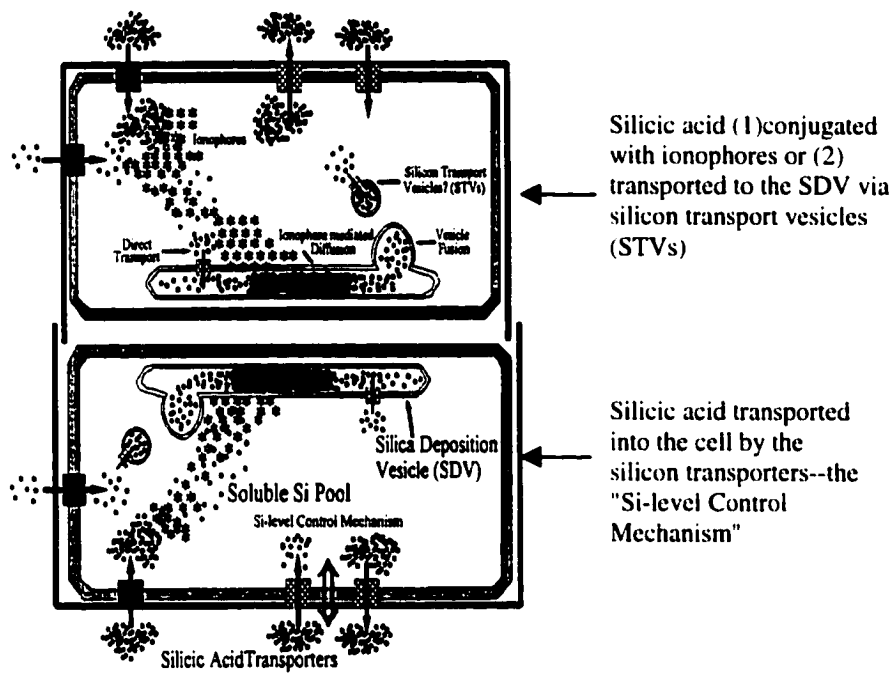


**Figure 9.** A schematic diagram of how silicic acid is first transported into the diatom cell and how the silica species is delivered hypothetically to the SDV.

## D. The Elusive Silica Species Used for Biosilicification

While much has been deduced in the field of biosilicification, one area that remains a mystery is the mechanism in which the silicic acid the organism uptakes from the extracellular environment is able to remain soluble at neutral pH until the SDV is reached. As is well known in silica chemistry, the kinetics of silica polymerization from silicic acid is greatest at pH 7 (19). It therefore remains a mystery on how a diatom for example is able to concentrate silicic acid intracellularly and prevent the silica species from prematurely condensing. Evidence has been suggested that a stable carrier or conjugate of silicic acid may be formed intracellularly prior to oligomerization in the SDV (20).

Carole Perry and colleagues have done much work in this area and have focused in the recent years on silicon catecholates since catechol-silicate complexes have been implicated in biosilicification in higher plants. In their study, Perry and Loton synthesized a range of catecholate salts with the molecular formula,  $(M^+)_2[Si(C_6H_4O_2)_3] \cdot xH_2O$ , where  $M^+$  is  $Li^+$ ,  $Na^+$ ,  $K^+$ ,  $NH_4^+$  and  $Et_3NH^+$ , and studied their breakdown and subsequent oligomerization under approximately neutral conditions (pHs ~7-8) (21). The catechol complexes were found to be stable at pH ~ 8 but quickly decomposed to the monomeric  $Si(OH)_4$  form at pH 7 and this was then followed by rapid condensation to silicon dioxide. TEM and CRYOTEM were used to identify the size and nature of the particles forming the

aggregates and it was found that the aggregates were influenced foremost by the ionic radii of the counterions of the catecholate (22).

Studies in diatoms also suggested the presence of a carrier or ionomer of silicic acid that not only stabilized the silica species but also could transport it through an oily layer, much like the membrane bilayer of the SDV. The chemical structure of the ionomer is still to be identified and is currently being pursued at UCSB.

## E. Biomimetic Synthesis of Silica

For quite some time inorganic chemists and material scientists have pursued the field of biomimetic silica synthesis. Because scientists differ in what they define as biomimetic, varying strategies exist. As mentioned earlier, Carole Perry has used the laboratory synthesized silicon catecholates as precursors to organize silica on hydroxylated biological surfaces, such as cellulose (22). Here, she used a preorganized organic template that could potentially hydrogen bond to monosilicic acid at pH 7 and "nucleate" the polymerization of silica. On the other hand, Steve Mann, Geoffrey Ozin and their coworkers have studied the morphogenesis of silica shapes using the influences of vesicles and surfactants to sculpt the inorganic shapes and patterns, mimicking the SDV in the natural systems (23).

The term biomimetic can also apply to syntheses that are done at ambient pressure and pH. While Ozin has been successful in creating patterns of crystalline aluminophosphate very similar to that of diatoms and radiolarians, the syntheses were done at extremely high temperatures, unlike the physiological temperatures of 15-25°C (24). Recently, Pinnavaia published a route for producing mesoporous materials at ambient conditions (pH, temperature). He and his coworkers used a neutral diamine bola-amphiphile to create porous lamellar silicas of vesicular particle morphology and unusually high surface area and pore volume (25).

Pinnavaia's one step approach to produce these porous lamellar structures eliminated the need for a separate pillaring step to introduce porosity into lamellar structures. It must be kept in mind though, that since diamines are basic groups, it is doubtful that the pH of Pinnavaia's system remained neutral throughout the entire reaction.

While chemists and materials scientists have invested much effort into producing silica structures biomimetically, many challenges evidently still exist. The mechanisms that nature uses to create such wonderful silica infrastructures can help gain further insights on how to biomimetically organize silicon based materials.

- (1) Belcher, A.M., Wu, X.H., Christensen, R.J., Hansma, P.K., Stucky, G.D., Morse, D.E. *Nature*, **381**, 56-58 (1996)
- (2) Falini, G., Albeck, S., Weiner, S., Addadi, L. *Science*, **271**, 67-69 (1996)
- (3) Perry, C.C., Williams, R.J.P., Fry, S.C. *Jour. Plant Physiol.*, **126**, 437-448 (1992)
- (4) Kröger, N., Bergsdorf, C., Sumper, M. *EMBO*, **13**, 4674-4683 (1994)
- (5) Kröger, N., Bergsdorf, C., Sumper, M. *Eur. Jour. Biochem.*, **239**, 259-264 (1996)
- (6) Kröger, N., Lehmann, G., Rachel, R., Sumper, M. *Eur. Jour. Biochem.*, **250**, 99- 105 (1997)
- (7) Voronkov, M.G. in *Silicon Chemistry*, Corey, J.Y., Corey, E.R., Gaspar P.P. (eds), Ellis Horwood Ltd., Chichester, (1993) pp 145-152
- (8) Hecky, R.E., Mopper, K., Kilham, P., Degens, E.T. *Marine Biology*, **19**, 323-331 (1973)
- (9) Swift, D.M., Wheeler, A.P. *Jour. Phycology*, **28**, 202-209 (1992)
- (10) Lobel, K.D., West, J.K., Hench, L.L. *Marine Biology*, **126**, 353-360 (1996)
- (11) Lobel, K.D., West, J.K., Hench, L.L. *Jour. Mat. Sci. Letters*, **15**, 648-650 (1996)
- (12) Kröger, N., Deutzmann, R., Sumper, M. *Science*, **286**, 1129-1132 (1999)



- (13) Bütschli, O. *Z. Wiss. Zool.*, **69**, 235-286 (1901)
- (14) Schwab, D.W., Shore, R.E. *Nature*, **232**, 501-502 (1971)
- (15) Harrison, C.C., Lu, Y. *Bulletin de l'Institut Océanographique*, **14**, 151-158 (1994)
- (16) Harrison, C.C. *Phytochemistry*, **41**, 37-42
- (17) Vrieling, E.G., Gieskes, W.C., Beelen, T.P.M. *J. Phycology*, **35**, 548-559 (1999)
- (18) Hildebrand, M., Volcani, B.E., Gassmann, W., Schroeder, J.I. *Nature*, **385**, 688-689 (1997)
- (19) Iler, R.K. *The Chemistry of Silica*, Plenum Press, New York, 1979
- (20) Weis, A. & Herzog, A. in *Biochemistry of Silicon and Related Problems* (Bendz, G. & Lindqvist, I. Eds.), Plenum Press, New York, pp.109-125 (1978)
- (21) Harrsion, C.C., Loton, N. *Jour. Chem. Soc. Faraday Trans.*, **91**, 4287-4297 (1995)
- (22) Perry, C.C., Yun, L. *Jou. Chem. Soc. Faraday Trans.*, **88**, 2915-2921 (1992)
- (23) Mann, S., Ozin, G.A. *Nature*, **382**, 313-318 (1996)

(24) Oliver, S., Kuperman, A., Coombs, N., Lough, A., Ozin, G.A. *Nature*, **378**, 47-50 (1995)

(25) Tanev, P.T., Pinnavaia, T.J. *Science*, **271**, 1267-1269 (1996)

## CHAPTER 1: The Organic Matrix of the Sponge Spicules

Because of the difficulty of producing an enormous amount of silica from diatoms, other species were initially studied in conjunction. Samples of sponges were sent to Professor Dan Morse from England and in observing their structures by SEM, the intricacy and beauty of the silica skeletons were seen to be easily comparable to that of the diatom frustules. The previous sponge literature demonstrated how little was actually known on the biosilicification process in these organisms except that that within the glassy needles or "spicules", an organic core was visualized (1). As mentioned earlier, the researchers named this occluded organic component the axial filament and it was thought that this filamentous core may act as a direct template for silica mineralization. At the time, it was not known whether the axial filaments were composed of both proteins, glycoproteins or polysaccharides. It was also not known as to what exactly occurred at the interface between the organic filament and the silica species.

Wanting to know more about sponge biosilicification, I turned to a colleague in Prof. Morse's lab, James Weaver, and asked if he knew of a species of sponge that we could collect off the Santa Barbara coast to study and furthermore from which we could extract spicules with relative ease. He immediately named the species, *Tethya aurantia* whose more familiar name is the "Orange Puffball Sponge" (Figure 10). Besides the abundance of these sponges off the coast, the other important advantage to this species that he mentioned was that the animal's

skeleton was primarily composed of only one type of spicule and from individual to individual collected, there would be no or little difference in spicule composition and morphology.

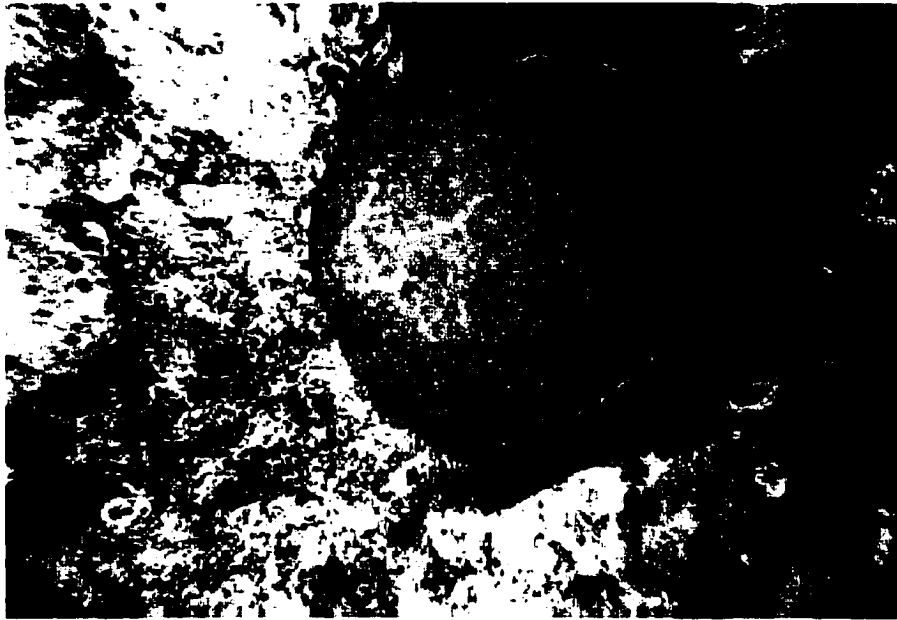
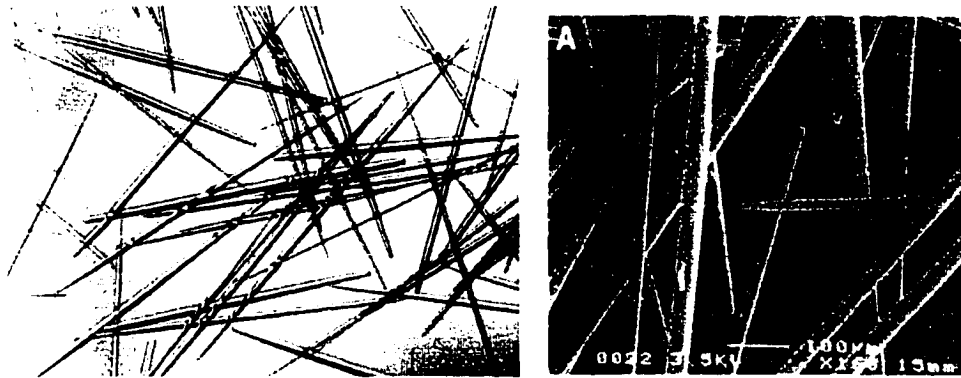


**Figure 10.** The *Tethya aurantia* or more commonly known as the "Orange Puffball Sponge"

Specimens of the sponge, *Tethya aurantia*, were collected at 17m depth off Santa Barbara County, California (latitude 34°25.331'N, longitude 119°57.142'W). Sponges were washed of debris, dissected into cubes and bleached with sodium hypochlorite (NaOCl) until all of the organic material had dissolved. The bleached material that had settled in the process was collected by filtration and cleaned further by first washing with Milli-Q (Millipore) purified water followed by an overnight treatment with a mixture of concentrated nitric

and sulfuric [ $\text{HNO}_3/\text{H}_2\text{SO}_4$  (1:4)] acids. Acid-insoluble material was then observed by both light and scanning electron microscopy. The samples were sputter coated with gold for SEM and examined with a JEOL JSM 6300F equipped with a cold cathode field-emission source operated at a beam energy of 3.5kV. As is shown in Figures 11a and 11b, the sponge skeleton is composed almost entirely of long needles whose dimensions are approximately 2mm in length and 30 $\mu\text{m}$  in width.



**Figures 11a, b:** Light microscopy (11a) and scanning electron micrographs (11b) of the cleaned spicules extracted from *Tethya aurantia* by oxidation and acid treatment.

The light microscopy images display the beauty and transparency of the spicules and in Figure 12, the axial filament running down the middle of the glassy matrix is easily discernible. More interesting though is the observation that the bifurcation of this spicule clearly follows that of the axial filament. This image only strengthens the hypothesis that the axial filament acts as a direct template for silicification in the *Tethya aurantia*.

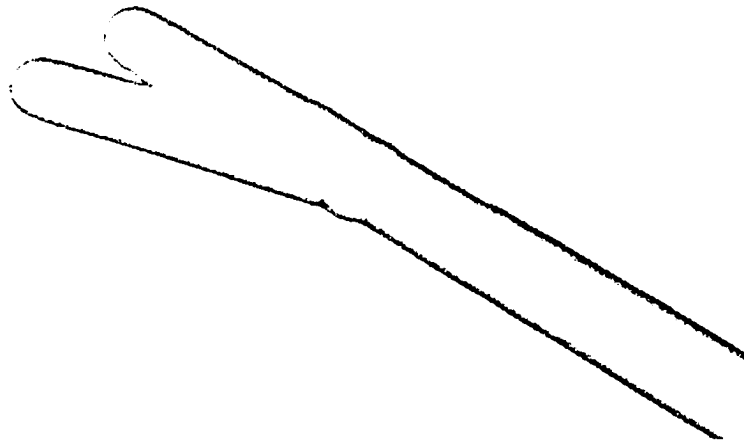


**Figure 12.** An image of a bifurcated spicule whose axial filament clearly appears to direct the final orientation of the silica.

One of the other key reasons that the *Tethya aurantia* proved to be the ideal biosilicate to study was that its yield of silica showed to be an amazing 75% of its total dry weight (Table 3) (2). Since many of the sponges collected were approximately 8 g in dry weight, about 6 g of silica could be collected per sponge. From this, approximately 6 milligrams of protein was collected (.1% organic by dry weight) and from a biochemist's standpoint, 6 mgs is a substantial amount of protein to work with.

**Yields of silica spicules, filaments, and filament protein from  
*Tethya aurantia***

Material	Weight	Yield %*
Sponge (wet)	20.0	100
Sponge (dry)	7.3	100
Spicules	5.5	75.3
Filaments	0.0058	0.11
Protein	0.0053	0.10

\*Yield was calculated relative to sponge dry weight as 100%. (Dry weight of the sponge was ca. 35% of the live wet weight). *reprinted from Shimizu et al., PNAS (1998)*

**Table 3.** Yields of spicules and proteins from *Tethya aurantia*

Both wide and small angle X-ray analyses were done on the spicules but no discernible peaks were found indicating that the needles were composed of completely amorphous SiO<sub>2</sub>. <sup>29</sup>Si MAS (magic angle spinning) NMR (nuclear magnetic resonance) studies were also done on the spicules and the spectra demonstrated mainly broad Q<sup>4</sup> and Q<sup>3</sup> peaks with a small Q<sup>2</sup> peak. This showed that the spicules were composed of highly condensed amorphous silica.

Although no long or short range order of the intact spicules was observed by x-ray, the possibility arose that perhaps none was seen because of the highly condensed nature of the silica. Therefore, spicules were partially etched with 1M hydrofluoric acid for 5 minute intervals of times ranging from 5 to 60 minutes.

The samples were then washed extensively with nanopure water, air-dried and gold sputter coated for SEM. As is shown in Figure 13, upon partial etching for 15 minutes in strong hydrofluoric acid, relative order is observed in the form of nanospheres with a size range of 80-100 nm.

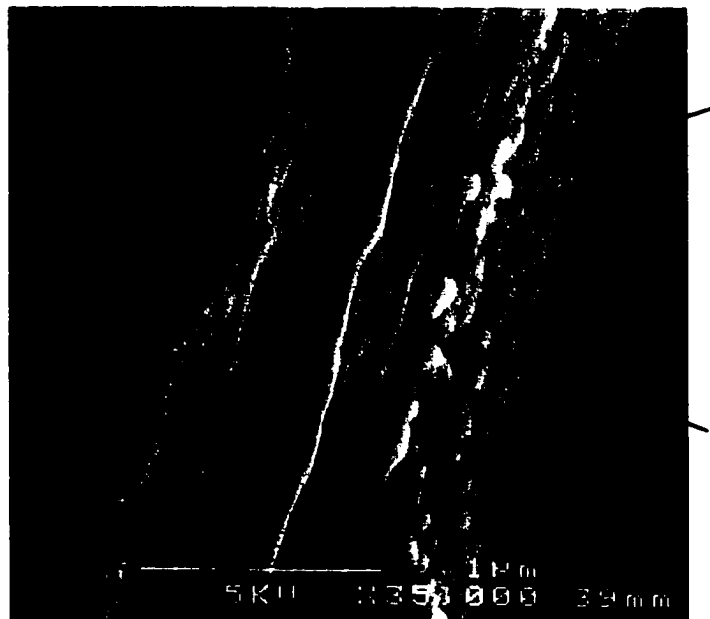


**Figure 13.** Partial etching of the spicules with HF revealed microspheres of silica, ranging in size from 80-100 nm.

When a similar treatment was performed on regular coverslip glass slides, no such micro- or nanospherelike structure was seen. However, as mentioned earlier, previous SEM images of intact diatom frustules had demonstrated organized arrays of silica spheres on the order of 80-100 nm and nanospheres



were also produced in Kroeger's *in vitro* experiments with the silaffins (Figure 5). Both wide and small angle x-ray analyses of the partially etched spicules did not however show any low or high angle peaks.

When the oxidized and acid-cleaned spicules were treated with buffered HF ( 1M HF/4M NH<sub>4</sub>F) (pH ~ 5) to completely dissolve the silica, intact axial filaments were isolated (Figure 14). After an overnight treatment of the spicules with HF, the solution was dialyzed against successive changes of 4-8L of nanopure, milli-Q water. The filaments then were collected by mild centrifugation and air-dried. For SEM, the filaments were first gold sputter-coated to prevent charging. As is shown in Figure 14, while the filaments have the dimension of the spicule (~2mm), their widths are approximately only 1.5  $\mu$ m.



**Figure 14.** Axial (Silicatein) filaments extracted from the core of the spicules upon HF treatment of the glassy needles. The silicatein filaments are approximately 2mm in length and 1.5-2  $\mu$ m in width.

While both SEM and atomic force microscopy (AFM) of the dried filaments

failed to lend any insight into its molecular organization, small angle x-ray diffraction data of a collection of the filaments oriented on a glass coverslip revealed a periodicity of 17.2nm as shown in Figure 15 (2).

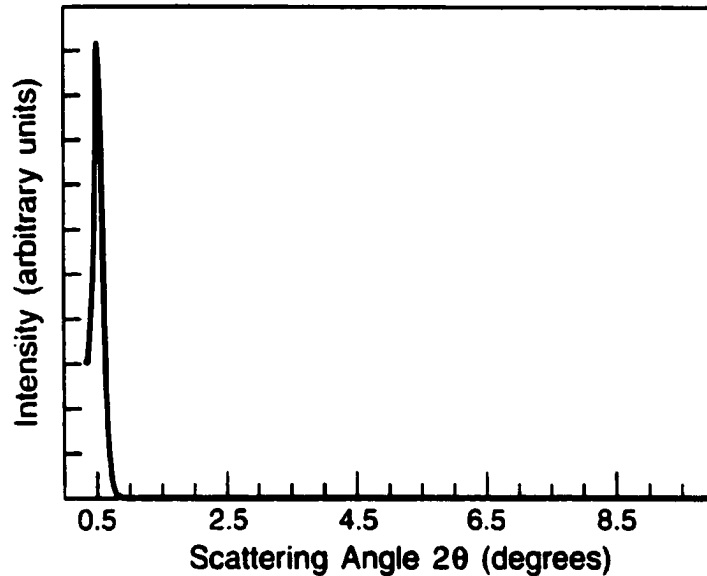


**Figure 15.** Small angle x-ray scattering data of the axial filaments (~2mg/ml) air dried on a glass coverslip after extensive dialysis against nanopure, milli-Qwater.

Since the general diameter of a globular protein (of approximately 25,000-30,000 daltons in molecular weight) can be on the order of  $\sim 50 \text{ \AA}$ , a periodicity of 17.2nm could correspond to a regular array of three globular proteins along the length of the axial filament. Because of the dimensions and overall lack of stiffness of the filament, it was virtually impossible to mount a single filament on a glass fiber for x-ray measurement.

The organic filaments were solubilized in sodium dodecyl sulfate (SDS) polyacrylamide (PAGE) sample buffer [2% SDS, 20% glycerol, 20mM

Tris-HCl, pH 8, 2mM EDTA, 80mM DTT, bromphenol blue] at 100°C for 10 minutes and

run electrophoretically on a 12.5% SDS PAGE gel. 10 µg of protein was loaded onto the gel and after staining with Coomassie brilliant blue R250, three protein bands corresponding to molecular weights of 29, 28, and 27 kDa were observed; these proteins were designated silicateins (silica proteins)  $\alpha$ ,  $\beta$ , and  $\gamma$  respectively (Figure 16). Densitometric analyses showed that these proteins existed in the relative proportions  $\alpha:\beta:\gamma = 12:6:1$  (2) and as also displayed in Table 4, the amino acid compositions of the three proteins are highly similar.

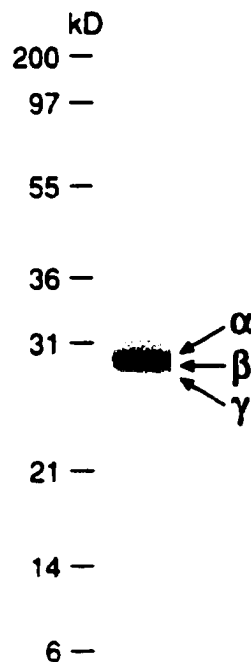


**Figure 16.** Gel electrophoresis of the filaments after dissolution in the SDS-PAGE sample buffer. The arrows indicate the positions of the bands

corresponding to silicateins  $\alpha$ ,  $\beta$  and  $\gamma$  (29, 28 and 27 kDa respectively)

It was also determined from amino acid analysis that approximately 91% of the silicatein filaments was protein.

<b>Composition, Mole %</b>				
<b>Residue</b>	<b>Filament Proteins</b>	<b>Silicatein <math>\alpha</math></b>	<b>Silicatein <math>\beta</math></b>	<b>Silicatein <math>\gamma</math></b>
Asx	11.8	12.5	12.4	12.7
Thr	4.8	6.7	4.8	4.3
Ser	10.9	13.0	12.3	11.8
Glx	8.8	8.8	10.2	10.3
Pro	3.2	2.1	2.2	2.5
Gly	12.7	15.2	14.8	13.7
Ala	9.2	9.6	10.0	10.6
Val	6.4	4.1	5.7	6.3
Met	2.3	1.6	1.2	1.0
Ile	4.3	4.0	3.9	4.0
Leu	6.0	7.0	6.2	7.4
Tyr	7.9	6.3	6.6	7.8
Phe	2.8	2.4	2.5	2.2
His	1.3	0.8	0.5	0.4
Lys	4.4	3.3	3.7	3.8
Arg	3.1	2.6	2.9	1.6

**Table 4.** Amino acid compositions of the intact filaments and of the individual silicatein subunits

While the silicatein filaments were amazingly stable in buffered HF and at extremely low pHs, the filaments disintegrated completely above the pH of 10. After solubilization in mild alkaline conditions such as 10mM NaOH, the alkali was removed by dialysis against nanopure water at 4°C. During this process, the silicatein subunits remained in solution. However, at concentrations above 1

mg/ml, if the silicatein monomers were left at pH 7 for more than 12 hours, a white precipitation was seen at the bottom of the sample tubes, indicating that the silicatein subunits did in fact have a high affinity for aggregating with each other.

Through a collaboration with Dr. Katsuhiko Shimizu, we were able to get the amino acid sequence of the major protein, silicatein  $\alpha$ . This was accomplished by first purifying silicatein  $\alpha$  by first excising the protein band out of a gradient gel and obtaining N-terminal sequences. The partial amino acid sequences were then used to design degenerate oligonucleotide primers for amplification of the corresponding cDNA. The amino acid sequence of silicatein  $\alpha$  was then derived from the full-length 1360 base pair (bp) cDNA (Figure 17) (2). Dr. Shimizu furthermore found that the sequence contained 112 amino acid residues upstream from the N-terminus of the mature protein within which was a typical 17-residue signal peptide that is thought to mediate secretion. Since biosilicification had been previously shown to occur inside the silicon deposition vesicle (SDV), the existence of a signal peptide is not surprising.

**A**

```

1 MYLGLTVVLC VLGAAIGEPM POYEFKEEWQ LWKKQHDKSY STNLEELEKH
51 LVWLSNKKYI ELHNANADTF GFTLAMNHLG DMTDHEYKER YLTYTNSKSG
101 NYTKVFKREP WMAYPETVDW RTKGAVTGIK SQGDCGASYA FSAMGALEGI
      .....
151 NALATGKLTY LSEQNIIDCS VPYGNHGCKG GNMVVAFLYV VANEGVDDGG
      .....
201 SYPFRGKQSS CTYQEQRGA SMSGSVQINS GSESDLEAAV ANVGPVAVAI
      .....
251 DGE SNAFRFY YSGVYDSSRC SSSSLNHAMV ITGYGISNNO EYWLAKNSWG
      .....
301 ENWGELGYVK MARNKYNQCG IASDASYPTL

```

**Figure 17.** The amino acid sequence of the mature form of silicatein  $\alpha$ .

The astonishing feature of the silicatein  $\alpha$  was the discovery of its high homology to a class of cysteine proteolytic enzymes and specifically, human cathepsin L. Alignment of silicatein  $\alpha$  with human cathepsin L revealed that 45% of the corresponding amino acids were identical between the two full-length proteins; 52% were identical when the regions corresponding to the mature protease and silicatein  $\alpha$  were compared. The percentage rose to 75% when residues of biochemical identity or similar side chains were analyzed. Compared to other members of the papain-like protease family, such as papain and cathepsin B, there was less identity--39 and 28 % identity respectively. (Figure 18)



backbones. It was inexplicable at first as to why proteins extracted from silica would be so similar to this particular class of enzymes.

Despite the high similarity in sequence between silicatein  $\alpha$  and human cathepsin L, there was one critical difference. Among all proteolytic enzymes, it is well known that the active site is composed of three key amino acids which form what is defined as the "catalytic triad". Among cysteine proteases, the three amino acids are cysteine which performs the actual hydrolysis of the peptide backbone, histidine and asparagine or aspartic acid (Figure 19). As is shown in Figure 18 in, while the asparagine and the histidine are conserved in silicatein  $\alpha$ , the cysteine has been modified to a serine, making the silicatein's "active site" actually mimic that of a serine protease.

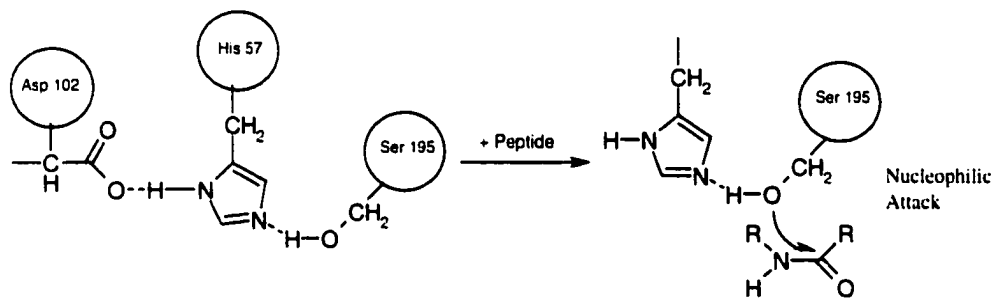


**Figure 19.** The catalytic triad of cysteine proteases (3).

The sequence of silicatein  $\alpha$  was also different from that of human cathepsin L in its singular clusters of hydroxyl amino acids, including Ser-Ser-Cys-Thr-Tyr, Ser-Ser-Arg-Cys-Ser-Ser-Ser-Ser and two Ser-Xaa-Ser-Xaa-Ser



sequences (Figure 18). These hydroxyl rich domains could be regions where monomers of  $\text{Si}(\text{OH})_x(\text{OR})_y$  would interact with the proteins by hydrogen bonding and facilitate in the nucleation of silica at the inorganic organic interface. This is in direct correlation to the hypotheses that had initially been proposed by Hecky (Figure 2).

(1) Shore, R.E. *Biol. Bulletin*, **143**, 689-698

(2) Shimizu, K., Cha, J., Stucky, G.D., Morse, D.E. *Proc. Natl. Acad. Sci. U.S.A.*, **95**, 6234-6238 (1998)

(3) *Principles of Biochemistry*, 2nd edition, A.L. Lehninger, D.L. Nelson, M.M. Cox (eds), Worth Publishers, New York, NY, 1993 p.226

## CHAPTER 2: Activity of the Biological Proteins

Because of silicatein  $\alpha$ 's high homology to human cathepsin L, the silicateins were first assayed for proteolytic activity. The filaments were first solubilized in 10mM NaOH for 10 minutes and then extensively dialyzed at 4°C against Tris buffer (25mM, pH 6.8). The silicateins were reacted with N $\alpha$ -Benzoyl-L-Arginine 7-Amido-4-Methylcoumarin, a fluoregenic substrate used often to measure proteolytic activity for papain and trypsin. The silicateins demonstrated no enzymatic activity toward this particular substrate or any of the other amino acid derivatives that were tested. In order to further verify that the negative result was not due to lack of correct substrate specificity, bovine serum albumin (BSA) was also mixed with the silicateins  $\alpha$ ,  $\beta$ , and  $\gamma$  for 1 hour at room temperature and also at 37°C. The entire reaction mixture was then electrophoresed on a 12% SDS PAGE gel to see if any degradation of the BSA had occurred. But after staining with Coomassie brilliant blue R250, the only bands observed were that for the intact BSA and silicateins. These two results thus demonstrated that at least under the conditions in which the silicateins  $\alpha$ ,  $\beta$ , and  $\gamma$  had been produced, the proteins demonstrated no proteolytic activity. One hypothesis for this may be that it is because the catalytic cysteine of human

cathepsin L is replaced with a serine in the silicatein  $\alpha$ , thereby altering the active site enough to prevent hydrolysis of peptide backbones.

A different hypothesis may lie in the fact that as stated in Chapter 1, despite the high percentage of similarity between human cathepsin L and silicatein  $\alpha$ , there do remain some essential differences. One as mentioned before is the run of hydroxyl residues in silicatein  $\alpha$ . Another striking contrast between the two proteins is shown in their respective hydrophobicity/hydrophilicity plots, (Figure 20. courtesy of Dr. Katsuhiko Shimizu and Camille Lawrence).

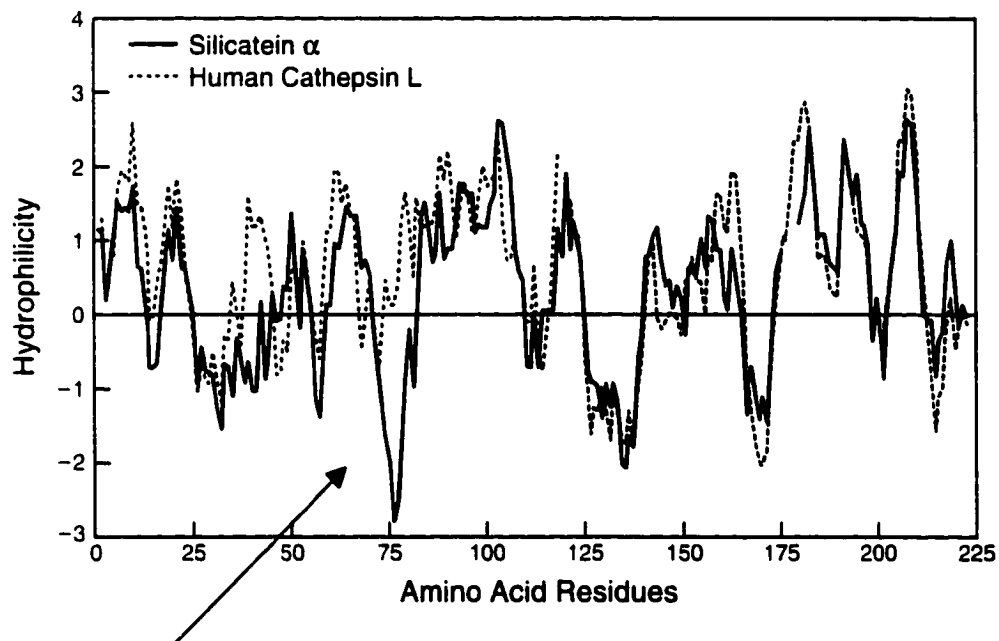


**Figure 20.** Hydrophilicity/hydrophobicity plots for both human cathepsin L and silicatein  $\alpha$ . As is shown by the arrow, there is one region in silicatein  $\alpha$  that is distinctly much more hydrophobic than that in silicatein  $\alpha$ .

It is clearly discernible in the plots that a distinct hydrophobic domain exists in silicatein  $\alpha$  and not in human cathepsin L. A computer model of silicatein  $\alpha$  is shown in Figure 21.

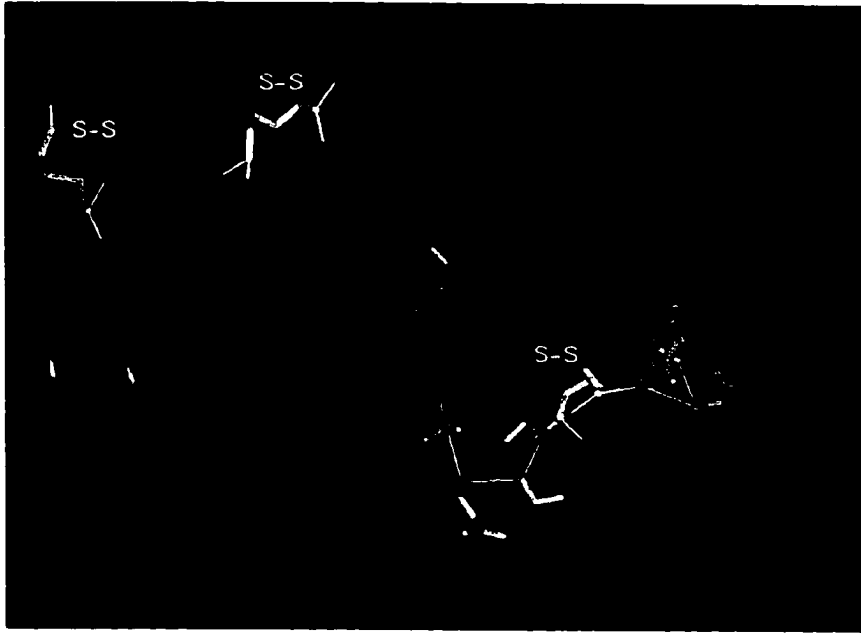


**Figure 21.** A model of silicatein  $\alpha$  computationally designed on the known, crystallographic structure of human cathepsin L. (courtesy of Camille Lawrence & Prof. Dan Morse)

The red  $\alpha$ -helical domain represents the "hydrophobic patch" that is found astonishingly on the exterior of silicatein  $\alpha$ . Since most hydrophobic regions of proteins exist within their globular structures, it is postulated that this area is responsible for interactions between the silicatein monomers and in producing the

macroscopic filaments shown in Figure 14. Yet it is also conceivable that this hydrophobic patch may prevent such hydrophilic substrates such as amino acids or a peptide backbone from entering the active site of the protein, thereby explaining their inability to act as proteases.

Because of the silicatein  $\alpha$ 's high homology with human cathepsin L, it was still very feasible that the silicateins would display a catalytic activity when given the correct substrate. Since the proteins were tightly encased in a silica matrix, silicon based substrates were obvious candidates. It was mentioned earlier that one hypothesis of the mechanism of biosilicification was that once monosilicic acid was transported into the cell, it was then converted to a stable organosilicon compound. Although Perry had used silicon catecholates in her *in vitro* studies, these were not attempted because of their apparent instability at pH 7 (1). Silicon catecholates are stable at pH 8 but when the pH is reduced to 7, they spontaneously hydrolyze to  $\text{Si}(\text{OH})_4$  and undergo rapid condensation to form  $\text{SiO}_2$ .

In deciding which organosilicon compound to try, alkoxides immediately came to mind since it is well known in sol-gel chemistry that silicon alkoxides must undergo hydrolysis prior to any condensation to silica (2). Since the silicateins had an active site that seemed poised to perform hydrolysis, silicon alkoxides seemed like good candidates as possible substrates. Furthermore, many silicon alkoxides are highly stable at neutral pH, although this does depend on the length and bulkiness of the alkyl chain. Hydrolysis of these compounds is therefore usually accomplished by adding either acid or base catalysts.

One of the most common silicon alkoxide used is tetraethylorthosilicate (TEOS)  $[\text{Si}(\text{OCH}_2\text{CH}_3)_4]$  and at pH 7, this compound can remain stable for days to weeks depending on the water concentration. In order for  $\text{SiO}_2$  to be produced from TEOS, hydrolysis to  $\text{Si}(\text{OH})_4$  must occur prior to condensation to silicon dioxide (Figure 22).

### Silicon Alkoxide Chemistry

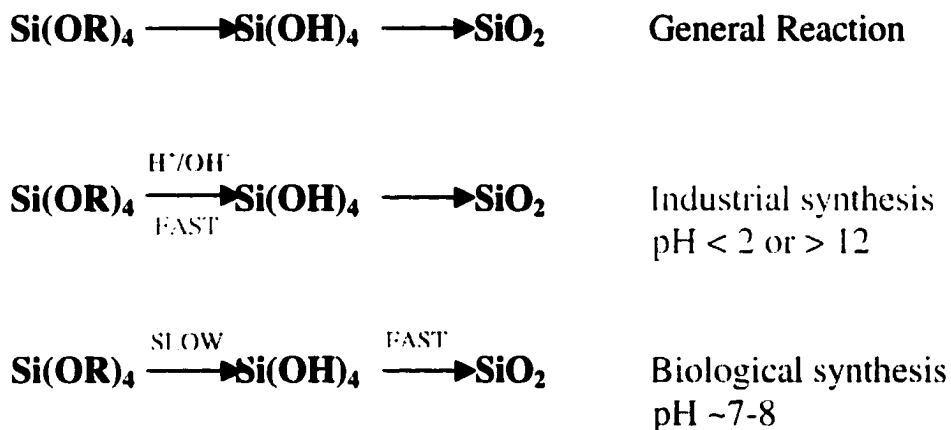


**Figure 22.** The general reaction scheme of silicon alkoxides. Acid or base catalysts are usually required for alkoxides where  $\text{R} = (\text{CH}_2)_n\text{CH}_3$ ,  $n \geq 1$ .

During synthesis of highly ordered, mesoporous silica, pHs below 2 or above 12 are generally utilized (3). It is useful to remember though that while hydrolysis of the silicon alkoxide is very fast at these extreme pHs, condensation to  $\text{SiO}_2$  is slow due to either complete protonation of the hydrolyzed species at

low pHs or to the highly negatively charged  $\text{SiO}_4^{4-}$  species that form at high pHs. This is in direct contrast to that of neutral pH where the hydrolysis of the alkoxide is extremely slow but condensation from  $\text{Si}(\text{OH})_4$  to  $\text{SiO}_2$  occurs rapidly. At pH 7, the hydrolysis step is the rate limiting one.

The silicateins were reacted with TEOS in order to see if the proteins could catalyze the hydrolysis of the silicon alkoxide at neutral pH. The silicatein subunits were prepared by alkali treatment (10mM NaOH) of the silicatein filaments followed by extensive dialysis at 4°C against 50mM Tris-HCl, pH 6.8; the proteins were then brought to a final concentration of 0.26mg/ml. The protein concentrations were determined by reading the absorbance of the solutions at 280nm; it had previously been determined by Dr. Shimizu that an absorbance of 1.0 at 280nm corresponded to a silicatein concentration of approximately 1 mg/ml. Since the proteins sometimes aggregated and precipitated out in solution after a few days at 4°C, the silicateins were used immediately after dialysis was complete. 156 µg (total volume 600 µl) of protein was reacted with 1ml of TEOS (4.5 mmol) at room temperature and vigorously pipetted to create an initial completely emulsified mixture; the reactions were then allowed to continue for 15 minutes at room temperature with mild rotation. The rigorous mixing was performed initially in order to thoroughly mix the aqueous phase with TEOS so as to enable the diffusion of the silica substrate to the silicateins.

Within seconds of mixing the silicateins with TEOS, a precipitation was observed in the aqueous phase. The samples were centrifuged to collect the



sol-gel silica products and the pellets were washed three times with 1.5 ml of 95% ethanol to remove any unreacted TEOS. Control experiments included using other proteolytic enzymes, such as papain (a cysteine protease) and chymotrypsin (a serine protease), non-enzymatic proteins such as bovine serum albumin (BSA) and buffer alone. The silica precipitates were hydrolyzed to monomeric silicic acid with 1M NaOH for 10 minutes at 95°C. Samples were also prepared where the precipitates were not hydrolyzed by base so as to calculate any residual TEOS that could not be efficiently removed with three washes of 95% ethanol.

The samples were then diluted and the released silicic acid was quantified using the ammonium molybdate reaction (Appendix 1). Absorbance readings were done at 810nm and standard curves were made with aliquots of TEOS resuspended in 10ml dimethylsulfoxide (DMSO).

The results of reacting the various proteins with the silicon alkoxide TEOS at pH 7 are shown in Table 5 (4).

---

**Silicatein subunits catalyze polymerization of silica**

---

<b>Protein</b>	<b>Polymerized Si, nmol</b>
<b>A. Silicatein subunits</b>	
Native	214.0 ± 2.0
Denatured	24.5 ± 2.0
Bovine Serum Albumin	42.1 ± 0.7
Papain	22.9 ± 1.0
Trypsin	16.2 ± 2.6
(None)	10.2 ± 1.3
<b>B. Recombinant silicatein</b>	
Native	140.0 ± 6.2
Denatured	8.8 ± 1.9
(None)	6.7 ± 2.1

---

Proteins in 0.6ml of Tris-HCl buffer (25mM, pH 6.8) were incubated with 1 ml (4.5 nmol) of TEOS, and the polymerized silica was quantitated after centrifugation and hydrolysis as described. For experiment A, proteins at 0.3 mg; reaction for 15 min. For experiment B, proteins at 0.06 mg; reaction for 60 min.

---

**Table 5.** The amount of silica produced from reacting various proteins with TEOS at pH 7.

As is clearly demonstrated in Table 5, the nanomoles of silica produced in 15 minutes with the silicateins was significantly higher than that of the control

experiments. In experiment A, the total mixture of silicateins  $\alpha$ ,  $\beta$ , and  $\gamma$  were used; in experiment B, purified and reconstituted silicatein  $\alpha$  expressed from a cloned cDNA template in bacteria (courtesy of Dr. Yan Zhou) was used (4).

It is interesting that while chymotrypsin and papain have active sites similar to that of the silicateins, no catalytic activity with TEOS was displayed with these particular proteins. The catalytic activity of the silicateins was abolished when the proteins were heated at 100°C for 20 minutes, demonstrating that the activity is highly dependant on the native conformation of the protein. The silica that was produced using the silicateins was gel like and confirmed by both small and wide-angle x-ray scattering to be completely amorphous in nature.

The results in Table 5 were derived from biphasic TEOS and water solutions. Because of this, the values shown may be influenced by the amount of TEOS that actually diffused into the aqueous phase and was available as a substrate to the proteins during the reaction. When ethanol was added to the solutions in order to make a monophasic mixture, very little silica was produced upon reacting the silicateins with TEOS. This could be because the silicateins denatured in an excess amount of alcohol.

Two other silicon alkoxides, tetramethylorthosilicate (TMOS =  $\text{Si}(\text{OCH}_3)_4$ ) and tetrabutylorthosilicate (TBOS =  $\text{Si}(\text{OCH}_2\text{CH}_2\text{CH}_2\text{CH}_3)_4$ ) were reacted with silicateins  $\alpha$ ,  $\beta$ , and  $\gamma$  at neutral pH (50mM Tris-HCl, pH 6.8). Little or no difference was seen between the no protein control and the addition of silicateins when using these two silicon alkoxides as substrates. In the case of TMOS, this is

presumably because TMOS hydrolyzes instantly with the addition of water or buffer at pH 7 and no additional catalyst is therefore required. A possible explanation for the negative results with TBOS is that it simply was too large and bulky of a substrate for the silicateins. It could also be that TBOS was too hydrophobic to easily diffuse into the aqueous layer.

(1) Perry, C.C., Lu, Y. *Jour. Chem. Soc. Faraday Trans.*, **88**, 2915-2921 (1992)

(2) Brinker, C.J. & Scherer, G.W. *Sol-Gel Science: The Physics and Chemistry of Sol-Gel Processing*, Academic Press, San Diego

(3) Zhao, D., Yang, P., Huo, Q., Chmelka, B.F., Stucky, G.D. *Curr. Opin. Solid State Mat. Sci.*, **3**, 111-121 (1998)

(4) Strickland, J.D.H. & Parsons, T.R. *A Practical Handbook of Seawater Analysis* (Fisheries Research Board of Canada, Ottawa), 2<sup>nd</sup> Ed. (1972)

(5) Cha, J.N., Shimizu, K., Zhou, Y., Christiansen, S.C., Chmelka, B.F., Stucky, G.D., Morse, D.E. *Proc. Natl. Acad. Sci. U.S.A.*, **96**, 361-365 (1999)

## CHAPTER 3: The Template

In the native organism, the silicatein subunits were ordered into macroscopic filaments. While the exact organization of the three individual proteins ( $\alpha$ ,  $\beta$ , and  $\gamma$ ) along the filament is not known at this time, there is a periodicity to the silicatein filaments that corresponds to approximately 17 nm (1). It was mentioned in Chapter 1 that this could correlate to repeated units of approximately 3 globular proteins. The question arose as to whether the filaments themselves could also catalyze the polycondensation of silica from TEOS at neutral pH and if so, would it allow for constrained and organized silica growth directly around the filament.

The silicatein filaments were purified by treating the cleaned glass spicules with buffered HF (pH ~5) followed by extensive dialysis at 4°C against 25mM Tris-HCl, pH 6.8. The filaments were suspended in 25mM Tris-HCl, pH 6.8 to a final concentration of 0.5mg/ml and 0.6 ml of this was reacted with 1ml (4.5 mmol) of TEOS with gentle rotation at room temperature for 12 hours. The samples were then collected by centrifugation, washed with 95% ethanol 3 times to remove any residual TEOS, air dried and gold-sputter coated for SEM. The JEOL JSM 6300F was operated at a beam energy of 3.5 to 5.0 kV. Control experiments were also done with other insoluble organic matrices such as cellulose (Sigma) and purified silk fibers (extracted from cocoons). As is shown

in Figure 23, after 12 hours of reaction, the macroscopic filaments served as scaffolds to organize the deposition of silica from TEOS at neutral pH. Figure 23A shows a SEM image of the cleaned native filament occluded within the spicule and Figure 23B is an image of one of the filaments after the reaction with TEOS at pH 7 (2).

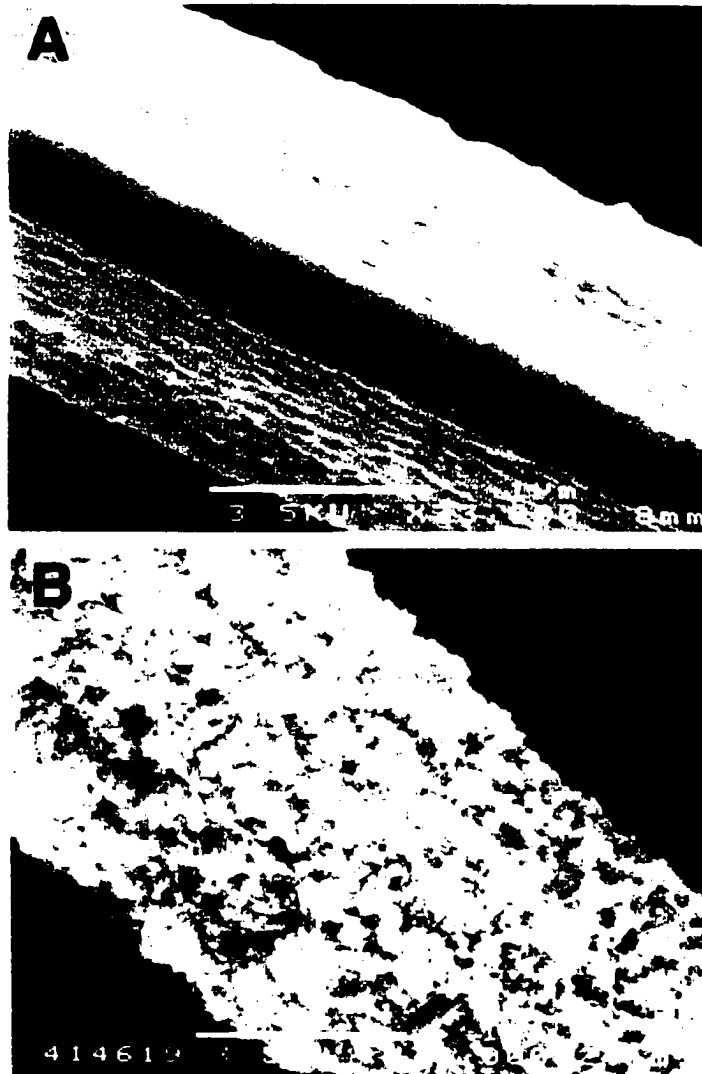


**Figure 23.** (A) A SEM image of a silicatein filament extracted from the spicules of *Tethya aurantia*. (B). A SEM image of one of the silicatein filaments after reaction with TEOS at pH 7 for 12 hours.

As is shown in Figure 23B, the silica growth appears to be controlled tightly at the organic interface. Presumably, this is because TEOS hydrolysis is occurring directly at the silicateins' active sites' on the surface of the filament, constraining



the polycondensation of silica to occur only around the template. This is demonstrated better when silicatein filaments were first air-dried before reacting with neat TEOS (no additional water was added to the system), thereby limiting the water to that of the protein hydration (Figure24).

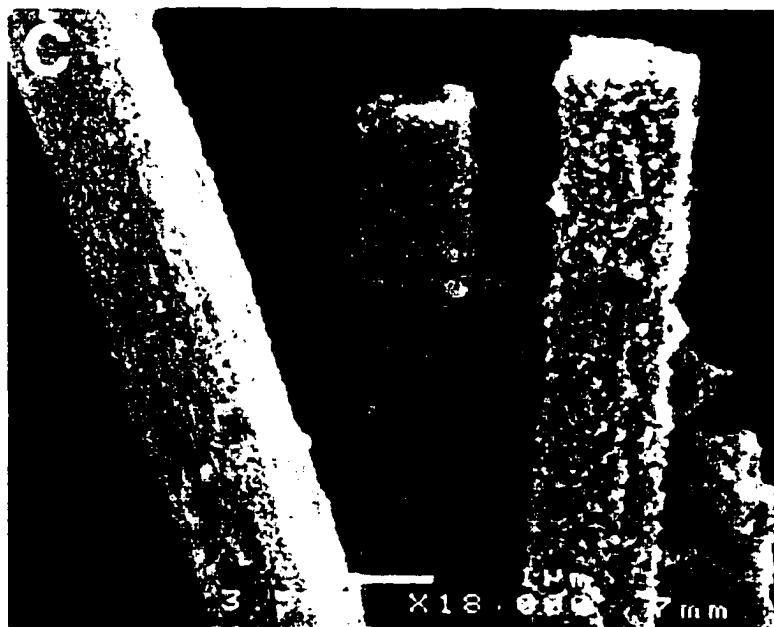


**Figure 24.** Air-dried silicatein filaments after reaction with TEOS for 12 hours. In this experiment, no additional water was added to the synthesis, limiting the water content to that of protein hydration.

In the absence of additional water, the dendritic growth of the silica was even more restricted to the silicateins' active sites at the filament surface since these were the only areas where any active hydrolysis of TEOS was taking place. This

therefore created a silica substructure that more strictly followed the longitudinal axis of the protein filament.

In the absence of the silicatein filaments, no polymerization with TEOS was observed at neutral pH during the course of the experiments. Neither silk nor cellulose (Figure 25) fibers exhibited any activity with TEOS under the same conditions, indicating that polymeric fibers with high surface densities of hydroxyl groups are not sufficient to accelerate or organize silica polymerization from TEOS at neutral pH. Figure 25E is a SEM image of a cellulose fiber and figure 25F shows a filament after reaction with TEOS at pH 7 for 12 hours.

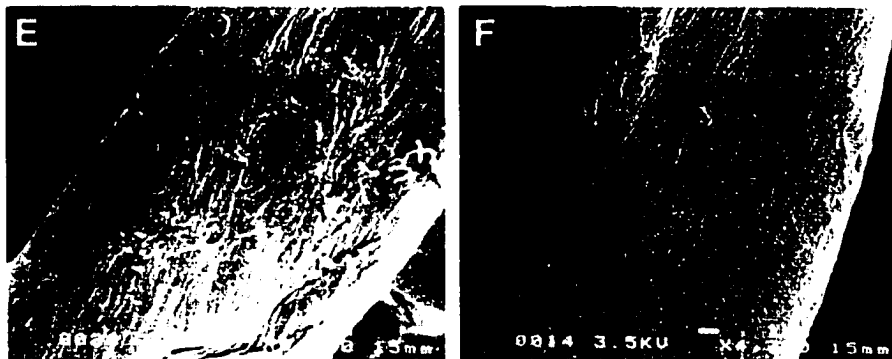


**Figure 25.** (E) A SEM image of a cellulose fiber (Sigma) (F) A SEM image of a fiber after reaction with TEOS at pH 7 for 12 hours.

With the collaborative assistance of Sean Christiansen and Prof. Brad Chmelka (Dept. of Chemical Engineering),  $^{29}\text{Si}$  magic-angle spinning (MAS) NMR was used to analyze the extent of polymerization of the siloxanes on the protein filaments. NMR spectra were acquired on a CMX-500 spectrometer (Chemagnetics, Ft. Collins, CO) operating at 11.7 Tesla and a  $^{29}\text{Si}$  frequency of

99.06 MHz referenced to tetramethylsilane. The single pulse spectrum was acquired for 22 hours with an 8.35- $\mu$ s single pulse and a recycle delay of 300 seconds, under conditions of magic-angle spinning at 3.5 kHz. Analysis of the products formed from TEOS (Figure 26) showed three inhomogeneously broadened peaks corresponding to  $Q^2$  ( $\approx$ -92 ppm),  $Q^3$  ( $\approx$ -101 ppm), and  $Q^4$  ( $\approx$ -110 ppm) siloxane species, indicative of a disordered, incompletely polymerized silica network often characteristic of the silica found in biological materials (2).

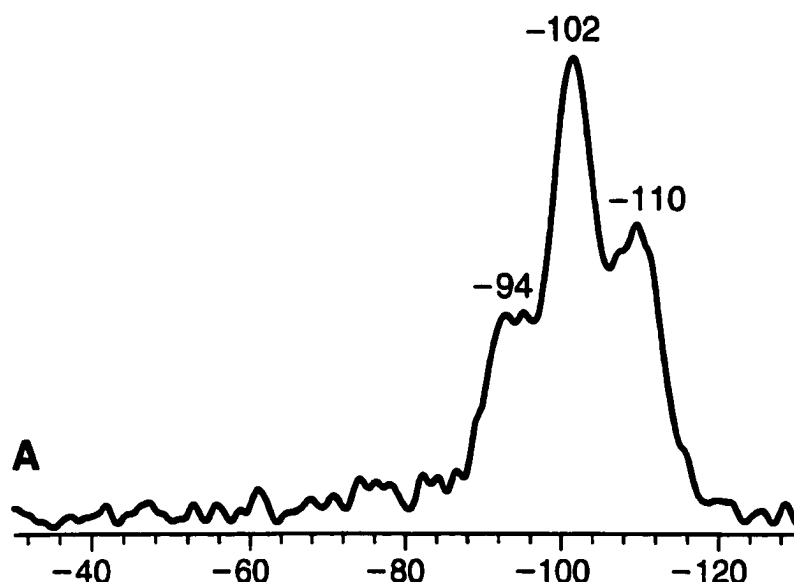
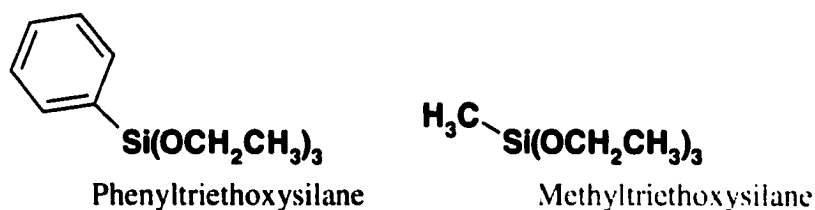


**Figure 26.**  $^{29}\text{Si}$  MAS NMR of the silicatein filaments after reaction with TEOS at pH 7. The filaments were collected by centrifugation and lyophilized for NMR analysis.

Samples of the silicatein filaments reacted with TEOS at neutral pH were air-dried on glass coverslips for both small and wide-angle powder x-ray analysis but the measurements only substantiated the amorphous nature of the silica as

seen by the  $^{29}\text{Si}$  NMR results.

The catalytic and structure-directing activities of the silicatein filaments were also evident with other organically substituted silicon alkoxides whose general structure is  $\text{R}-\text{Si}(\text{OEt})_3$ , where R can represent a phenyl or a methyl for example.



It is known from literature that silsequioxanes made from these various organo-silicon alkoxides have the capability of forming caged structures that can lead to interesting and novel optical properties. Such silicon based materials may offer more efficient optoelectronic materials with low-loss coupling to silicon-based semiconductors. Much research has therefore been invested in learning how to organize silisequioxanes from these starting precursors.

When phenyltriethoxysilane [ $\text{C}_6\text{H}_5\text{-Si}(\text{OEt})_3$ ] was provided as a substrate for the silicatein filaments, a polymerized product as before organized around the organic matrix (Figure 27).



**Figure 27.** The silicatein filaments after reaction with phenyltriethoxysilane at pH 7 for 12 hours.

This was confirmed by solid state  $^{29}\text{Si}$  cross-polarization MAS NMR analysis to be a silsequioxane since no  $\text{Q}^4$  resonance shift was seen. This result is consistent with the silsequioxane structure of the polymerized product since only three functional groups should be available for the formation of siloxane linkages. The cross-polarization results also exhibited the typical phenylsilisequioxane shifts: a  $\text{T}^3$  resonance at -79 ppm (shifted downfield by 20 ppm because of the phenyl substituent), a  $\text{T}^2$  signal at -70 ppm, and weak downfield  $\text{T}^1$  resonances (Figure 28) (3). Samples dried on glass coverslips for x-ray analysis once again showed the polymerized silsequioxane to be amorphous.

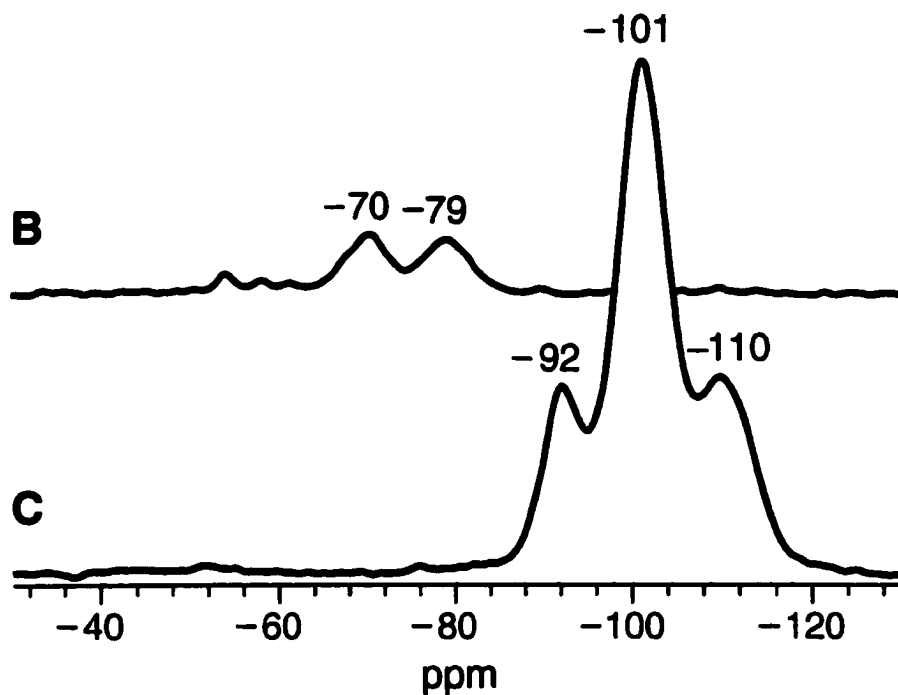


**Figure 28.** Cross polarization  $^{29}\text{Si}$  MAS NMR results of the silicatein filaments reacted with phenyltriethoxysilane (B) and TEOS (C) for 12 hrs at pH 7.

When the silicatein filaments were reacted with methyltriethoxysilane [ $\text{CH}_3\text{-Si}\equiv(\text{OEt})_3$ ], SEM images revealed only a very thin layer of siloxane product polymerized around the filaments. Most likely this is because the hydrolysis rate of methyltriethoxysilane is dramatically slower as compared to that of either TEOS or phenyltriethoxysilane.

As mentioned earlier, caged silsequioxane structures can demonstrate interesting optical properties such as blue luminescence. After the silicatein filaments were reacted with either the methyl- or phenyltriethoxysilane, they

were checked for fluorescence using a Fluoromax-2 spectrophotometer (Instruments S.A., Inc.) equipped with a xenon lamp as the light source. The filaments were scanned for fluorescence using excitation wavelengths ranging from 260 to 500nm at 10nm intervals as both a solid powder as well as a suspension in nanopure water. But under the described silica synthesis conditions, the phenylsilsequioxane coated filaments did not display any fluorescence at any wavelength.

In all of the reactions with the various alkoxides, those that had been terminated after 12 hours appeared to show order on the macroscopic scale but if the reactions were allowed to continue for more than 16 hours, much less order was observed. After 12 hours, any polymerized silica seemed to be relatively constrained to growing directly around the silicatein filaments but after 16 hours, the filaments seemed to have negligible roles in directing any new silica polymerization. Presumably, this is due to the fact that the *in vitro* experiments were not executed in membrane bound microenvironments as it is in the biological system where silica nucleation and condensation occurs in a silicon deposition vesicle. In order to create the beautifully organized needles of the *Tethya aurantia in vitro*, most likely it is important to use the filaments as the organic template and to also perform the syntheses in highly constrained spaces which can control the final macroscopic shape. As a final note, the puzzling phenomenon of how silica can grow from a 2 $\mu$ m in width filament to a needle 30 $\mu$ m in width is currently being studied in Prof. Morse's laboratory.

The experiments shown thus far demonstrate that when the silicateins  $\alpha$ ,  $\beta$ , and  $\gamma$  are assembled into macroscopic filaments, they can serve as scaffolds that spatially direct the synthesis of the polysiloxanes. These observations suggest that the biochemical mechanism of catalysis of polysiloxane synthesis mediated by the silicateins should be useful as a model for new routes to synthesis of silicon-based polymers and materials under environmentally benign conditions.

Both the condensation of silicon alkoxides promoted by the silicateins and the cleavage of peptides catalyzed by the proteases must proceed through an obligatory hydrolysis reaction, and both are known to be accelerated by general acid-base catalysis. This suggests that the mechanism of action of the silicateins may be related fundamentally to that of its homologous enzyme counterparts. The close relationship between silicatein  $\alpha$  and the proteolytic enzyme, human cathepsin L allowed us to propose that silicatein  $\alpha$  catalyzes the hydrolytic reaction of silicon alkoxides such as TEOS at neutral pH through the cooperative interaction of the serine and histidine side chains that occupy positions corresponding to the catalytically active, functionally related side chains in the proteolytic enzymes of both the cathepsin L (cysteine-histidine) and trypsin/chymotrypsin (serine-histidine). A hypothetical reaction scheme for the mechanism of the silicateins' hydrolytic activity is shown in Figure 29.



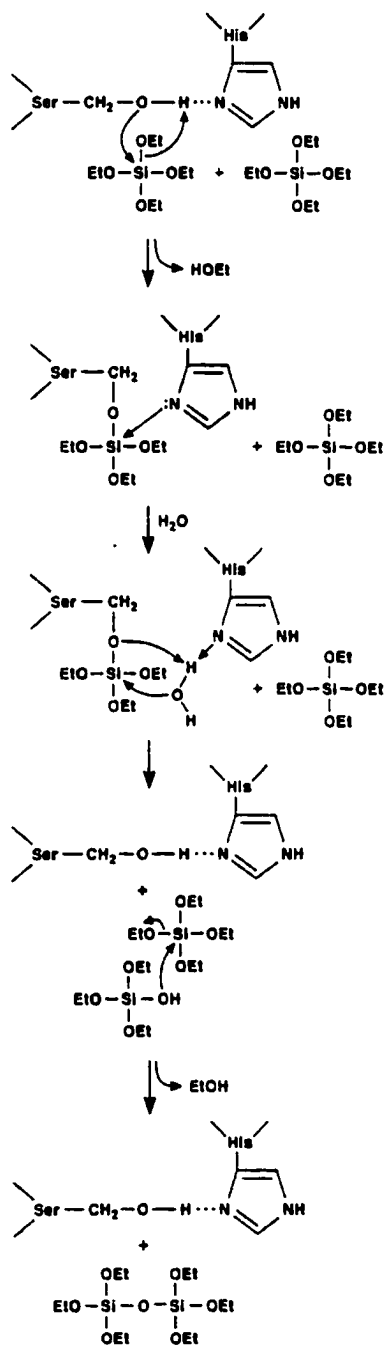


**Figure 29.** A proposed reaction mechanism of silicon ethoxide condensation catalyzed by silicatein, based on the well characterized mechanism catalysis by the Ser/His and Cys/His proteases.

Hydrogen-bonding between the imidazole nitrogen of the conserved histidine and the hydroxyl of the active-site serine was proposed to increase the nucleophilicity of the serine oxygen, potentiating its attack on the silicon atom of the substrate (Figure 29). Nucleophilic attack on the silicon displaces ethanol, forming a covalent protein---O---Si intermediate (potentially stabilized as the pentavalent silicon adduct via donor bond formation with the imidazole nitrogen). The addition of water completes hydrolysis of the first alkoxide bond. Condensation initiated by nucleophilic attack of the released Si---O on the silicon of the second substrate molecule then forms the disiloxane product. Catalysis of TEOS hydrolysis and subsequent condensation to silicon dioxide at pH 7 therefore may occur by the putative active site serine-26 interaction with histidine-165 to form a general acid/base catalyst.

In order to test this hypothetical scheme, Dr. Yan Zhou, a postdoctoral researcher in Professor Morse's group, proceeded to produce structural variants of the silicatein  $\alpha$  protein. Dr. Zhou targeted the proposed active site of silicatein  $\alpha$  and by site-directed mutagenesis produced variants in which the serine residue (with a hydroxymethyl side chain) at position 26, and the histidine residue (with an imidazole side chain) at position 165 were specifically replaced with an alanine residue (bearing a methyl side chain). The silicatein mutants were then purified and tested for catalytic activity. Quantitative comparison of the catalytic activities (Figure 30) supported the suggestion that both serine-26 and histidine-165 of the silicatein  $\alpha$  are required for efficient hydrolysis of the silicon alkoxide TEOS at neutral pH (4).

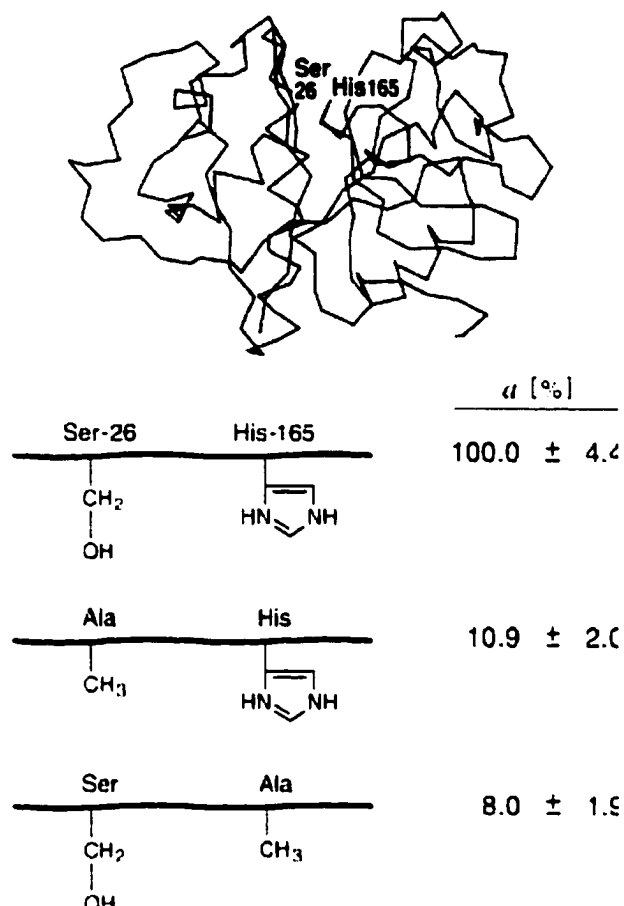


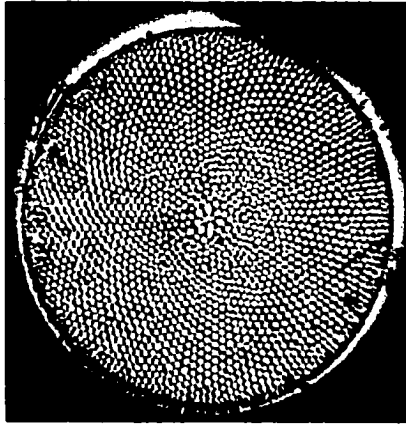
**Figure 30.** Values demonstrating the rate of activity of silicatein  $\alpha$  when either the Serine<sup>26</sup> or the Histidine<sup>165</sup> was replaced with the hydrophobic amino acid, alanine. (4)

The residual percentage of activity seen when either amino acid was replaced with alanine is most likely due to a basal amount of activity that is expected to occur from nucleophilic amino acids that are on the outer surface of

the proteins. In Table 5, the control proteins also demonstrated a basal level of activity that was approximately 10% of that of the silicateins.

- (1) Shimizu, K., Cha, J., Stucky, G.D., Morse, D.E. *Proc. Natl. Acad. Sci. U.S.A.*, **95**, 6234-6238 (1998)
  
- (2) Cha, J.N., Shimizu, K., Zhou, Y., Christiansen, S.C., Chmelka, B.F., Stucky, G.D., Morse, D.E. *Proc. Natl. Acad. Sci. U.S.A.* **96**, 361-365 (1999)
  
- (3) Smaïhi, M., Jermoumi, T., Marignan, J. *Chem. Mater.*, **7**, 2293-2299 (1995)
  
- (4) Zhou, Y., Shimizu, K., Cha, J.N., Stucky, G.D., Morse, D.E. *Angew. Chem. Int. Ed. Engl.*, **38**, 779-782 (1999)

## CHAPTER 4: Learning from Nature: Routes to Biomimetic Silica Synthesis



DIATOM

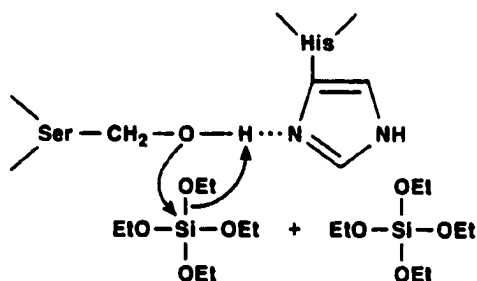


Synthetic Glass Sphere

As seen from the previous chapters, biological systems have the ability to form silica structures with highly controlled morphologies in ambient conditions by using proteins and polysaccharides as structure directing templates. This is in contrast to conventional laboratory syntheses that rely on extreme pH conditions and temperatures in order to induce the condensation of silica precursors into specific morphologies or patterned structures. Unlike diatoms, which can form their frustules at pH 7, synthesis of nano-, micro- and mesoporous silicon based materials are often done using silicon alkoxides at extremes of pHs (pHs less than 2 and greater than 12). The demonstration that silicatein can hydrolyze and condense TEOS to form silica structures with controlled shapes at ambient conditions seems promising in that we can adopt what was learned from the

biological system in order to biomimetically produce ordered silica structures. This would be accomplished using simple, laboratory synthesized polymers as the templates rather than complex proteins extracted from natural living systems.

It has been well established by researchers that in order to successfully produce ordered inorganic structures from an organic template, nucleation and subsequent growth of the inorganic material must start directly at the inorganic organic interface. This can be accomplished by strong charge charge or hydrogen bonding interactions and as demonstrated from the silicatein work, by catalytic or nucleophilic functionalities. In the silicatein model, it was the cooperativity between three, space-constrained amino acids that allowed for the rapid hydrolysis of silicon alkoxides, two of which is shown below.



Yet while the hydrolysis and subsequent condensation to silica was very rapid when the *soluble* silicateins were reacted with TEOS, little or no apparent morphological order was seen. In order to produce well defined materials therefore, the speed at which hydrolysis occurs is not as important as the process of hydrolysis and subsequent nucleation of silica at the organic interface.



This was demonstrated by the experiments done with the silicatein filaments and TEOS where the reaction times were as long as 12 hours but because hydrolysis occurred on a pre-organized template, the final product demonstrated morphological order as well.

In support of this theory then, it is not necessary to design polymers or peptides that exactly mimic the enzymatic site of the silicateins to create silica structures at ambient conditions. Functional groups such as sulfhydryls, hydroxyls or amines should have the capability of hydrolyzing a silicon alkoxide at neutral pH simply based on their nucleophilicity. As is shown schematically in Figure 31, an organic template could be designed such that nucleophilic groups such as the ones mentioned would be situated to hydrolyze the silicon alkoxides at the interface.

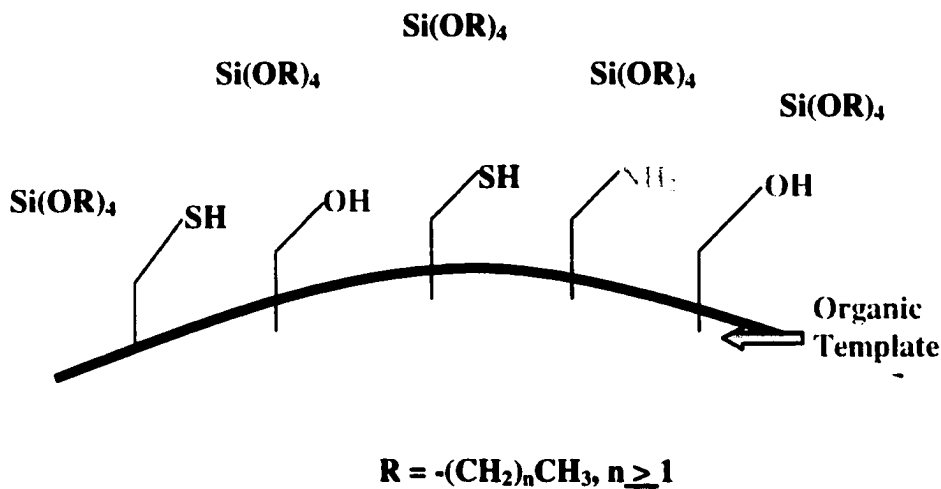


**Figure 31.** A schematic diagram of functional groups at the organic inorganic interface which could hydrolyze silicon alkoxides such as TEOS.

Although these functional groups are not as nucleophilic in nature as the active site serine residue of the silicateins, because they are more reactive than water, silicon alkoxides will be hydrolyzed and subsequently polymerized at the organic surface. If inorganic moieties that are normally stable at neutral pH like TEOS are used, hydrolysis of such compounds can be limited to the biological substrate allowing for stringent control at the organic inorganic interface. Lastly, the catalytic functionalities at the interface would also allow for silica syntheses to be done at neutral pH since no additional acid or base is necessary to hydrolyze the silicon alkoxide.

My ability to test these theories was facilitated by Prof. Tim Deming's discovery of the organonickel initiator, 2,2'-bipyridylNi(1,5-cyclooctadiene) [BpyNiCOD] that could synthesize high molecular weight block copolypeptides with well-defined size domains (1). The proposed mechanism of this initiator with the monomers, alpha-aminoacid-N-carboxyanhydrides (NCAs) is shown below in Figure 32.

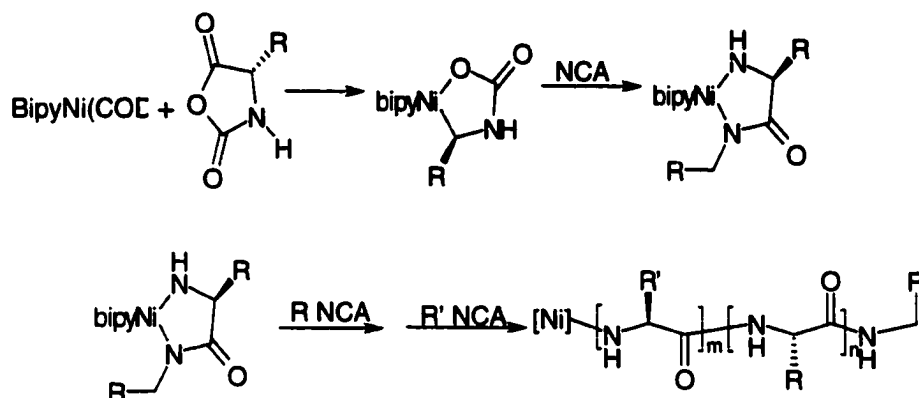


**Figure 32.** The synthesis of block copolypeptides using BpyNiCOD as the initiator.

BpyNiCOD is a zerovalent nickel organometallic compound which allows for the controlled, living polymerization of NCAs into complex polypeptide sequences and architectures. BpyNiCOD was synthesized from reacting equimolar quantities of 2,2-dipyridyl and Bis(1,5-cyclooctadiene)nickel(0) in tetrahydrofuran (THF) under inert atmosphere; once the two compounds were mixed, the solution turned to a violet-blue color. The initiator was left at 20-25°C in the dry box for at least 6 hours and then later transferred to the dry box 4°C refrigerator.

The block copolypeptides were produced through a living polymer synthesis by reacting the as made BpyNiCOD with the cyclized, suitably protected monomers, N-carboxyanhydride L-amino acids (NCAs). A general reaction for NCA synthesis is shown in Figure 33.

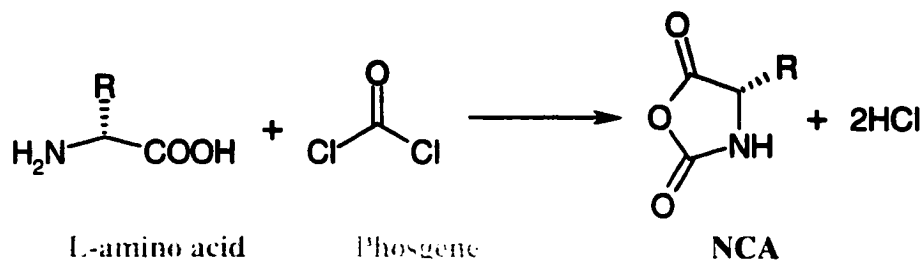
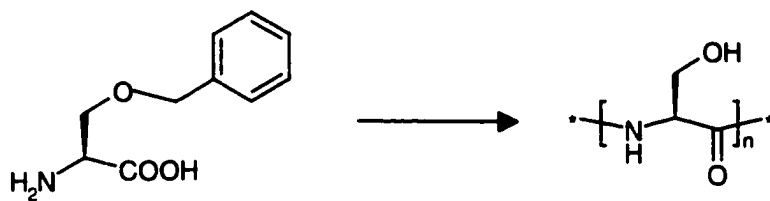


**Figure 33.** NCAs were synthesized by reacting suitably protected L-amino acids with a slight excess of phosgene.

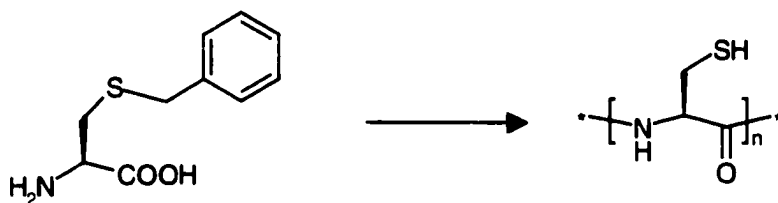
1.5 molar equivalents of phosgene was reacted with suitably protected L-amino acids in dry THF under a continuous flow of nitrogen. The syntheses were run for a few hours at 30-40°C until the solutions became clear and for a few more hours after that in order to ensure that no free amines (L-amino acids) existed. The THF was removed under vacuum and the NCA was recrystallized in the dry box. The NCA was first solubilized in a minimal amount of THF and recrystallized in hexane; usually only two recrystallizations were required. Any remaining HCl was detected by first dissolving a small amount of the NCA in concentrated nitric acid and then adding a drop of AgNO<sub>3</sub> and looking for any precipitate. For the amino acid, L-proline, the NCA had to be recrystallized at 4°C since the melting point of the NCA was low enough to cause an oil to form instead of crystals if done at room temperature. All of the pure NCAs were stored at 4°C until needed and were also characterized by FTIR and <sup>1</sup>H NMR. Figure 34

shows the protected L-amino acids used in order to make the NCAs for the corresponding polypeptides.



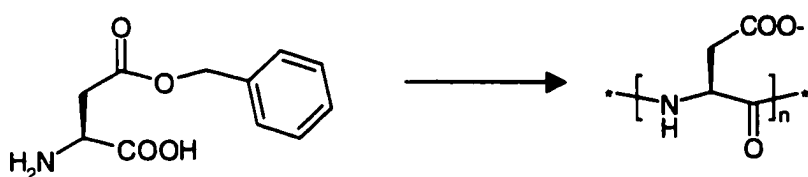
O-benzyl-L-serine

poly-L-serine



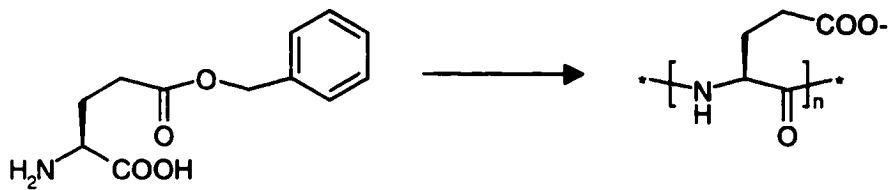
S-benzyl-L-cysteine

poly-L-cysteine



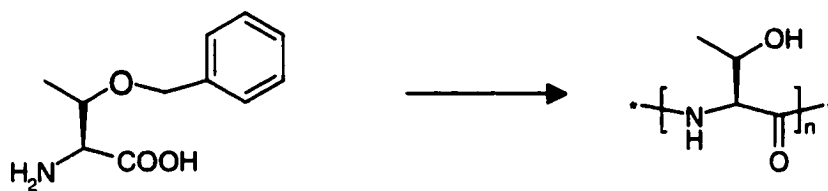
$\beta$ -benzyl-L-aspartate

poly-L-aspartic acid



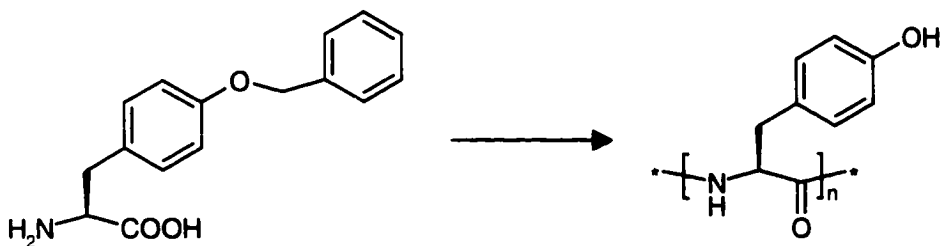
$\gamma$ -benzyl-L-glutamate

poly-L-glutamic acid



O-benzyl-L-threonine

poly-L-threonine



O-benzyl-L-tyrosine

poly-L-tyrosine

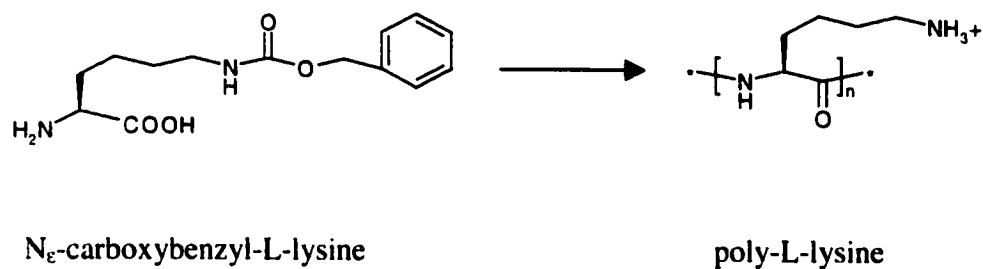
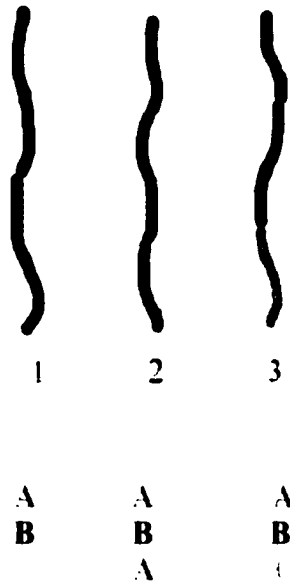


**Figure 34.** The protected L-amino acids used to make the NCAs are shown in the left column and the corresponding deprotected polypeptides are shown in the right column.

There are many different ways to design block copolymers and

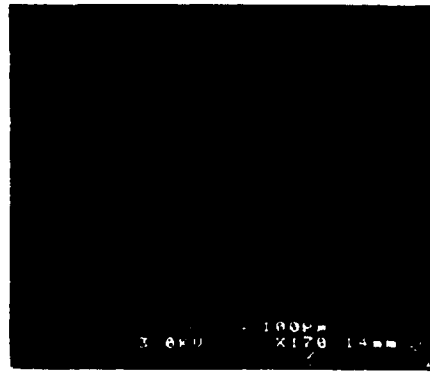


they can be synthesized as diblocks (1), ABA triblocks (2) or ABC triblocks (3) for example. One advantage to block copolymers have over random ones is the ease with which they can self-assemble into organized structures. This is more clearly observed in Figure 35 where lyophilized samples of a diblock copolyptide [poly (L-alanine<sub>30</sub>-L-lysine<sub>200</sub>)] and of a random copolyptide [15% L-alanine randomly dispersed in poly-L-lysine] are compared by SEM.





(A) poly-(L-alanine<sub>30</sub>-L-lysine<sub>200</sub>)



(B) 15% alanine dispersed randomly throughout poly-L-lysine

**Figure 35.** Scanning electron images of lyophilized samples of polypeptides. (A) shows that of a block copolyptide while (B) shows that of a random copolyptide.

This figure demonstrates that block copolypeptides have a higher degree of self-assembling as compared to that of random copolypeptides.

The initial task of strategically designing block copolypeptides was daunting since the amino acid pool is so large. The silicatein  $\alpha$ 's amino acid sequence could not be used as a starting point from which to work from since it was a complex sequence with no evidence of block-like character. However, it was possible to produce different block copolypeptides based on the biomimetic silica synthesis strategy discussed earlier which is shown in summary in Figure 36.

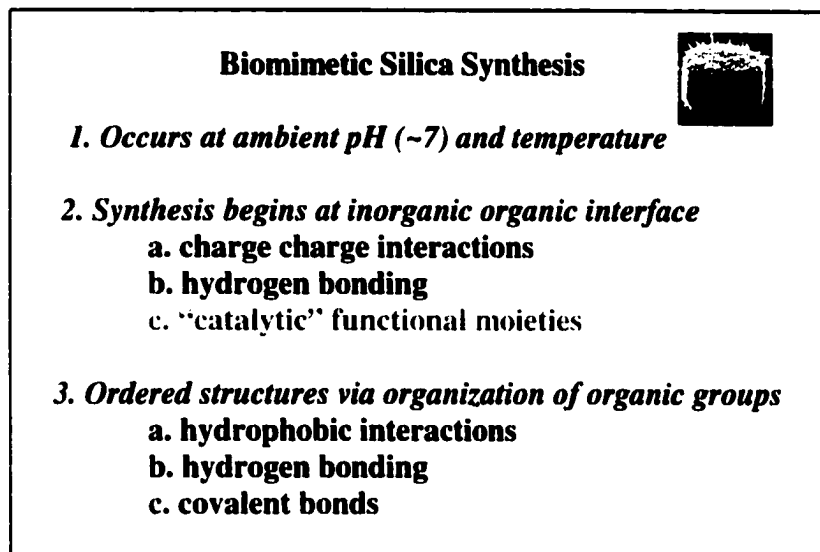
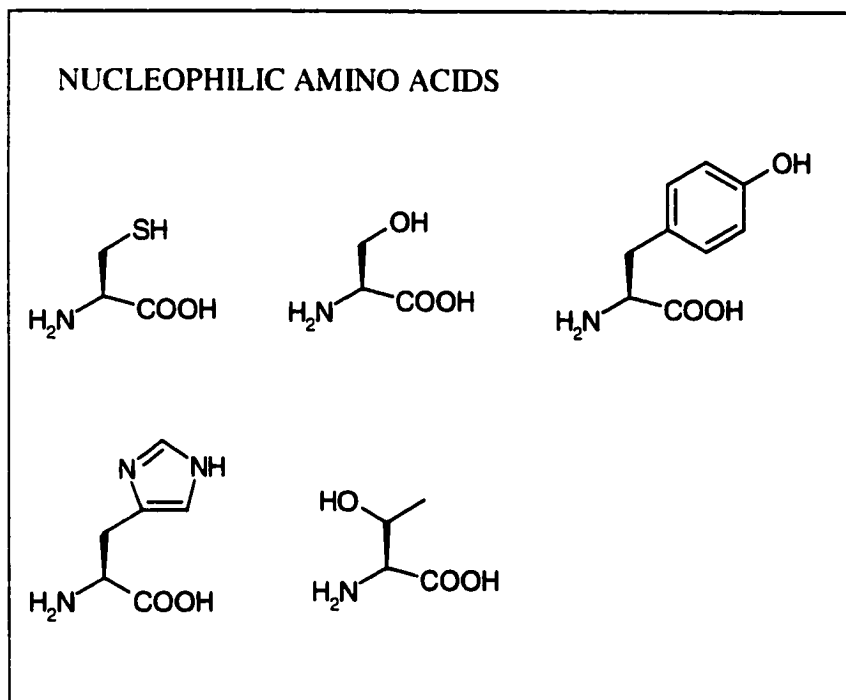


**Figure 36.** Summary of hypothetical scheme on biomimetically creating ordered silica structures.

Using this design strategy, the amino acid pool could be organized according to their respective functionalities such as shown below.



In order to test the capabilities of these amino acids in hydrolyzing TEOS at pH 7, polypeptides of the individual amino acids were synthesized. Polymers of various lengths determined by monomer (NCA) to initiator (BpyNiCOD) ratios were synthesized in DMF. For polypeptides made in THF, the amount of monomer that would have been used in DMF was further divided by 4 since it had earlier been observed that syntheses done in THF produced polypeptides whose final lengths corresponded to 4 times the expected lengths.

Synthesizing polymers of the nucleophilic amino acids proved to be a challenge because of their high level of insolubility in THF or DMF at molecular

weights beyond 2000-3000 daltons. The amino acid L-histidine posed even a greater challenge because of its imidazole group, only a protonated *Im*-benzyl-L-Histidine·HBr NCA salt could be made. Because protonated NCAs could not be used with any of the initiators, N-methylmorpholine (dried with CaH<sub>2</sub>) was used for the deprotonation of the Histidine·HBr NCA. Unfortunately, adding even a weak base such as N-methylmorpholine created a thick, viscous residue which by FTIR showed to be mainly polymer.

Due to all the above mentioned difficulties, some polypeptides were purchased from Sigma-Aldrich: poly-DL-serine (MW 5,000-15,000 daltons), poly-L-histidine(MW 5000-15,000) and poly-L-tyrosine (MW 10,000-40,000). Poly(L-threonine<sub>100</sub>) was synthesized in the lab and after many attempts, a very short oligomer of cysteine was also successfully produced.

The starting amino acid used to make the cysteine NCA was S-CBZ (carboxybenzyl)-L-cysteine and phosgene. The NCA was recrystallized in hexane with 50% yield. Instead of using BpyNiCOD as the initiator, very short oligomers of S-CBZ-L-cysteine was polymerized in THF using Co(PMe<sub>3</sub>)<sub>4</sub> (2) since this initiator was found in Prof. Deming's group to yield better results for synthesizing very short polymers. Although poly(S-benzyl-L-cysteine)<sub>50</sub> and poly(S-CBZ-L-cysteine)<sub>50</sub> immediately precipitated out in THF and DMF using BpyNiCOD, poly(S-CBZ-L-cysteine)<sub>30</sub> synthesized with Co(PMe<sub>3</sub>)<sub>4</sub> remained in solution with only a minor amount of precipitation. Since poly-L-cysteine also has the capability of forming disulfide bonds in air by oxidation, the polymer had to always be kept

under nitrogen in order to keep it reduced and soluble. It was therefore deprotected under a continuous flow of nitrogen by first dissolving the polymer in a small amount of trifluoroacetic acid (TFA) and then adding 1.5 molar equivalents of 33% HBr in acetic acid dropwise at 0°C. The TFA was removed by vacuum and the residue was transferred to a nitrogen box where it was first dissolved in a small amount of a 1:4 ratio of water to methanol. All solvents had been previously thoroughly degassed before use. The polymer was precipitated into diethylether and this process was repeated several times until all of the excess HBr was removed.

Once all of the polypeptides had been either purchased or synthesized, their hydrolytic capabilities with TEOS were tested for collectively. They were first solubilized in 50mM Tris-HCl buffer, pH 6.8 at 5 mg/ml. 1.5ml of TEOS was added to 0.5ml of the polymer solutions and the resulting biphasic mixture was vigorously agitated and then allowed to stand for 8 hours with no stirring, whereupon some of the TEOS had emulsified into the aqueous phase. After 8 hours, the silica precipitate was collected from the aqueous phase and washed three times with 95% ethanol. The SiO<sub>2</sub> formed was dissolved in 0.2M NaOH at 95°C for 1 hour in order to ensure that all of the silica had hydrolyzed to Si(OH)<sub>4</sub>. The amount of silica was then determined using the spectrophotometric molybdate assay as mentioned earlier (3). The results of mixing the nucleophilic polymers with TEOS at pH 7 are shown in Table 6.

## **Polypeptides**

<b>Composition</b>	<b>SiO<sub>2</sub> yield rate (μg/hr)</b>
1. poly(L-threonine) <sub>100</sub>	.011 ± .004
2. poly-L-histidine (Sigma)	.032 ± .002
3. poly-DL-serine (Sigma)	.045 ± .01
4. poly-L-tyrosine (Sigma)	.234 ± .008
5. poly(L-cysteine) <sub>30</sub> (N <sub>2</sub> )	.380 ± .005
-----	
6. poly-L-proline (Sigma)	.227 ± .001
7. poly(L-lysine) <sub>200</sub>	.008 ± .002
8. none	.005 ± .001

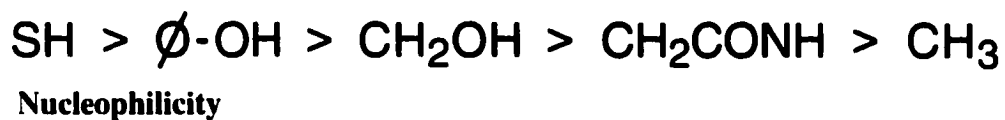
**Table 6.** Amount of silica produced from reacting the various polypeptides with TEOS at pH 7.

Poly(L-lysine)<sub>200</sub> was synthesized also from N<sub>ε</sub>-CBZ-L-lysine NCA and BipyNiCOD in THF. The polypeptide was deprotected in air using HBr in 33% acetic acid. Excess HBr and other acids were removed by dialysis at room temperature against 25mM Tris-HCl buffer, pH 7. As is seen from Table 6, poly-(L-lysine)<sub>200</sub> with its non-nucleophilic side chains was unable to hydrolyze a silicon alkoxide such as TEOS at pH 7. While it has been demonstrated by both Mizutani *et al* (4) and Kroger *et al* (5) that polycationic polymers can catalyze the polymerization of silica from stable solutions of silicic acid, it is clear from Table 6 that a positively charged polymer like poly-L-lysine cannot hydrolyze silicon alkoxides at pH 7.

Poly-L-threonine and poly-L-histidine produced little silica after 8 hours

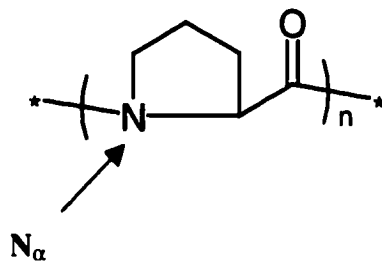
of reaction with TEOS at neutral pH; only a small amount of silica was observed in reacting the poly-D/L-serine with TEOS but this may be due in large part to the polymer's lack of chirality. It is interesting that although poly-L-histidine does contain a basic imine, it is not sufficient to catalyze the hydrolysis of TEOS. However, as a cautionary note, intra- or inter polymer chain hydrogen bonding between the imidazole groups may prevent the polypeptide from hydrolyzing the alkoxide.

From the data shown in Table 6, it can be inferred that the lower the pKa of the amino acid or the greater the Lewis acid characteristics of the side chain, the better the polypeptide acts as a catalyst for TEOS hydrolysis at pH 7 as is



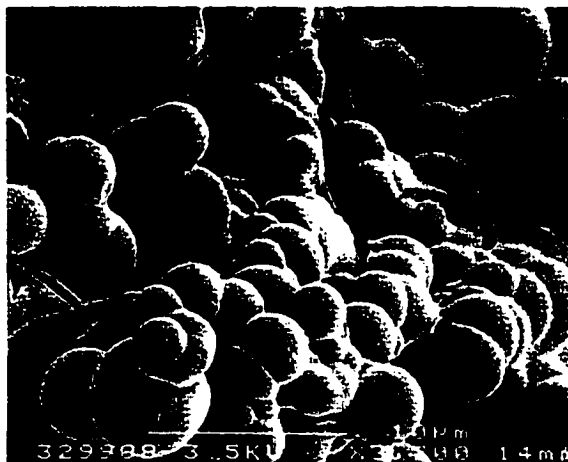
shown schematically here. This observation is not surprising given the fact that in the silicateins, the hydrolysis of TEOS is catalyzed by a serine residue whose Lewis acid characteristics are greatly enhanced by the cooperative interactions with other amino acids.

Table 6 also shows the results from another polypeptide, poly-L-proline and the polymer's repeating unit is shown below.



poly-L-proline

Although L-proline is not characterized as a nucleophilic amino acid, the data in Table 6 shows that it is quite capable hydrolyzing TEOS at pH 7. Even more surprisingly, while none of the other polymers yielded silica with any structured morphology, poly-L-proline produced clumps of silica "spheres" (Figure 37).



**Figure 37.** SEM image of the silica product formed after reacting poly-L-proline and TEOS at pH 7.



From all of the polypeptides tried, poly-L-proline was the only one that was capable of both catalyzing the hydrolysis of TEOS at pH 7 as well as creating some order to the final silica product. Although no direct evidence was found for how this occurs, one explanation for its catalytic properties could be that the  $N_{\alpha}$  of L-proline is a good nucleophile, presumably because its coordination with the three other carbons in the ring structure. The degree of order that was observed in the silica product from reacting poly-L-proline with TEOS may be due to the polypeptide's strong secondary helical structure. The other polypeptides shown in Table 6 have random secondary structures at pH 7; poly-DL-serine cannot form the  $\beta$ -sheet structure because of its racemic nature and poly-L-lysine can only form an  $\alpha$ -helical structure at pHs greater than 10. Yet in the case of poly-L-proline, the constrained peptide backbone forces the polymer to adopt a rigid helical structure and this may help in organizing the inorganic material. It may also be that in an emulsion system, poly-L-proline self-assembles into an organized scaffold due to both its rigid backbone structure as well as the amino acid's hydrophobic nature.

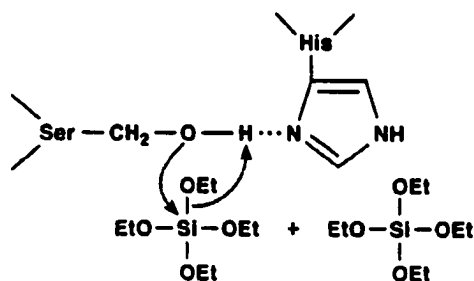
These previous experiments demonstrated that except for poly-L-proline, single amino acid based polypeptides cannot produce any ordered silica structures at pH 7 from TEOS. But before synthesizing diblock copolypeptides, mixtures of different homopolypeptides were first reacted with TEOS. As was discussed in the earlier chapters, the cooperativity between individual amino acids in the silicateins enabled the proteins to act as very efficient catalysts

for the hydrolysis of TEOS. 1.25 mgs of the different polypeptides were mixed with each other to a final volume of 0.5ml; the different combinations of polymers used are shown in Table 7. These were then mixed with TEOS (1.5ml; 6.72 $\mu$ moles) until the TEOS had emulsified into the aqueous phase. After 8 hours, any produced silica was both quantified by the molybdate assay as well as looked at by both light microscopy and SEM.

Polypeptide Mixture	SiO <sub>2</sub> yield rate ( $\mu$ g/hr)
1. poly-L-lysine + poly-L-threonine	.038 $\pm$ .006
2. poly-L-histidine + poly-L-threonine	.058 $\pm$ .006
3. poly-L-lysine + poly-DL-serine	.093 $\pm$ .001
4. poly-L-histidine + poly-DL-serine	.228 $\pm$ .008
5. poly-L-histidine + poly-L-tyrosine	.355 $\pm$ .005
6. poly-L-lysine + poly-L-cysteine (N <sub>2</sub> )	.543 $\pm$ .008
7. none	.004 $\pm$ .001

**Table 7.** The amount of silica produced from reacting combinations of different polypeptides with TEOS at neutral pH.

As shown in Table 7, the mixture of a cationic polymer such as poly(L-lysine<sub>200</sub>) and poly-L-threonine could still produce only negligible amounts of silica as well as poly(L-lysine<sub>200</sub>) and poly-DL-serine. Yet when poly-L-histidine and poly-DL-serine were mixed together and reacted in conjunction with TEOS for 8 hours, a substantial amount of sol-gel silica



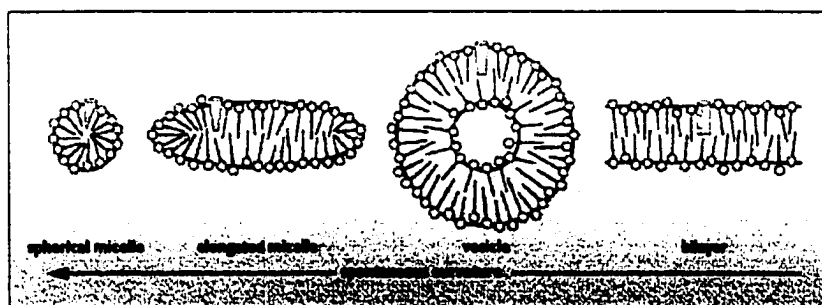
was produced. This is most likely due to the imine group on histidine hydrogen bonding to the hydroxyl of the serine residue, causing it to be a much more nucleophilic amino acid; this is not unlike that of the silicatein mechanism.

Although cooperativity between two separate polypeptide chains was demonstrated from some of the results shown in Table 7, when the silica produced from the polypeptide mixtures were looked at by SEM, no ordered silica structures were observed.

- (1) Deming, T.J. *Nature*, **390**, 386-389 (1997)
  
- (2) Deming, T.J. *Jour. Polymer Sci. Part A*, **38**, 3011-3018 (2000)
  
- (3) Cha, J.N., Shimizu, K., Zhou, Y., Christiansen, S.C., Chmelka, B.F., Stucky, G.D., Morse, D.E. *Proc. Natl. Acad. Sci. USA*, **96**, 361-365 (1999)
  
- (4) Mizutani, T., Nagase, H., Fujiwara, N., Ogoshi, H. *Bull. Chem. Soc. Japan*, **71**, 2017-2022 (1998)
  
- (5) Kröger, N., Deutzmann, R., Sumper, M. *Science*, **286**, 1129-1132 (1999)

## CHAPTER 5: Block Copolypeptide Design for Biomimetic Silica Synthesis

In order to create ordered structures of inorganic materials, the organic template must be organized as well. This has been demonstrated numerous times in mesopore synthesis as well as in the process of crystal nucleation. Our lack of success in creating ordered silica structures in the last chapter also stress the importance of using organized substrates as templates.



As shown above, polymers consisting of chemical domains whose functionalities differ in hydrophilicity and hydrophobicity can create a variety of self-assembled macroscopic structures ranging from micelles to vesicles to bilayers. One of the factors which control the self-assembly is the relative size of the head group compared to that of the hydrophobic tail (1). Block copolypeptides can be synthesized to form such self-assembled structures through the combination of different amino acids as shown in the following schematic (Figure 38A).

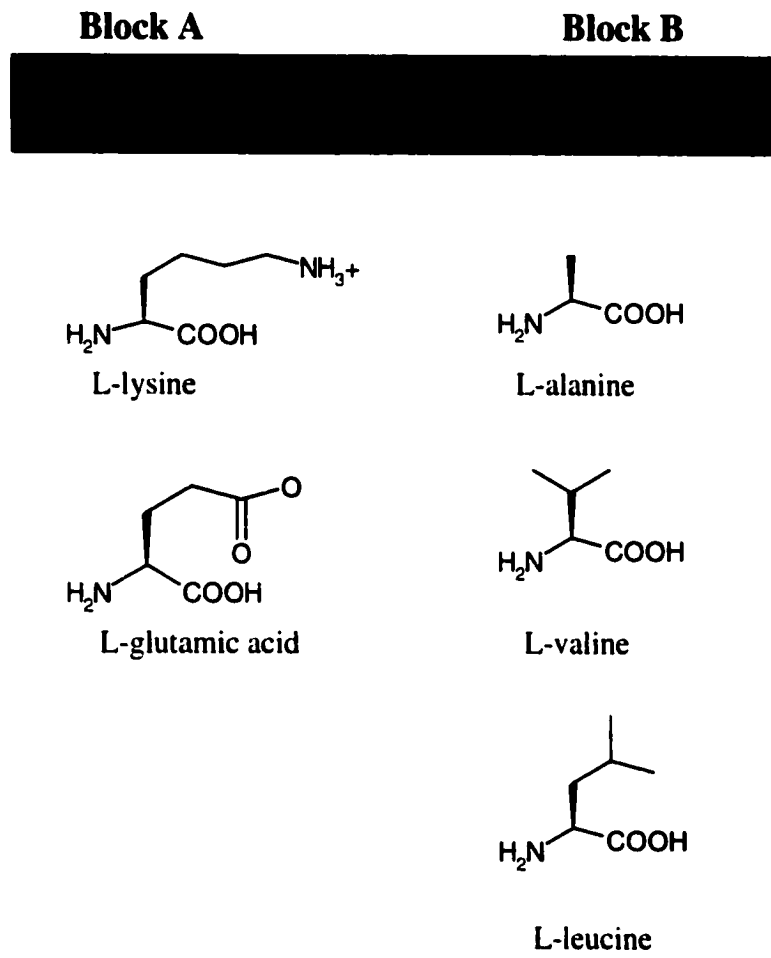


**Figure 38A.**

Block copolypeptides can be produced where block A is made up of charged amino acids (at pH 7) such as poly-L-lysine (cationic) and poly-L-glutamic acid (anionic) and where block B would be formed of hydrophobic amino acids such as L-alanine, L-valine, or L-leucine. Other amino acids which could also drive the

self-assembly of polypeptide chains are shown in the following diagram under "Block B" (Figure 38B).

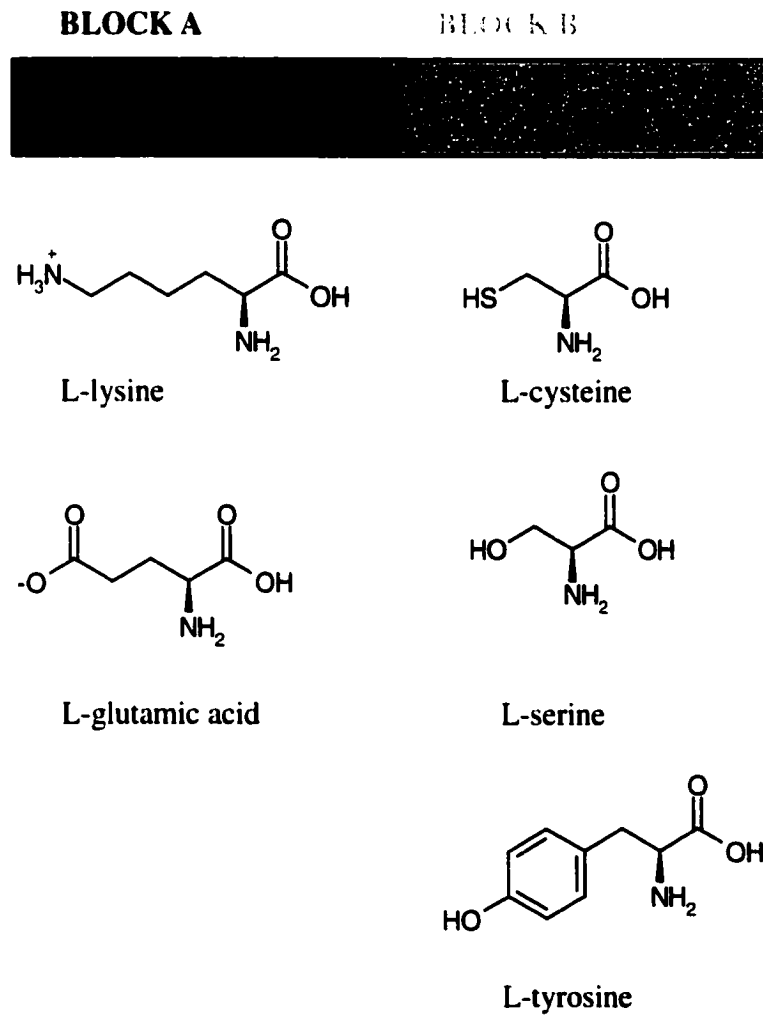
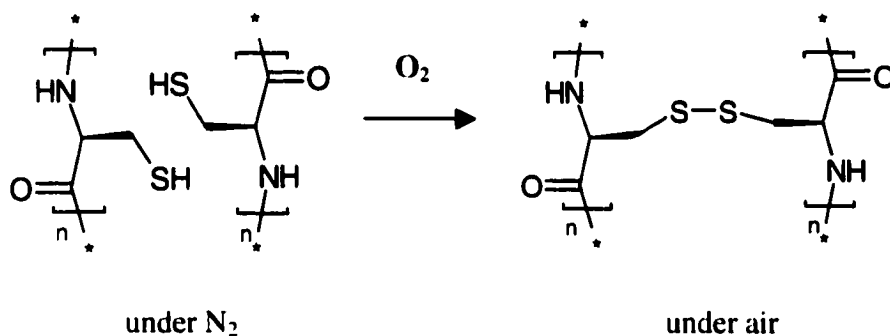


**Figure 38B**

By using these particular amino acids for block B, the polypeptide chains would self-assemble either through hydrogen bonding or in the case of a diblock with L-cysteine, covalent disulfide bridging upon oxidation of the sulfhydryl groups.



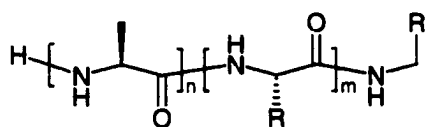
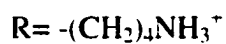
Under reducing conditions, L-cysteine remains in its natural sulfhydryl (-SH) form but upon exposure to air, the cysteines oxidize to form either intra- or inter-chain disulfide bonds.

Aside from their self-assembling properties, Figure 37B also depicts amino acids which have the capability of acting as catalysts for the hydrolysis of silicon alkoxides at pH 7. The dual role these amino acids could play provided an interesting array of amino acids from which to work from.

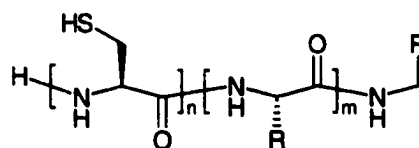


The following pages will describe in detail the diblock copolypeptides that were synthesized and tried. Block A was primarily made of either L-lysine or L-glutamic acid; this block was often termed the "solubilizing block" since it enabled the polypeptide that formed block B to remain soluble in either water or buffer at pH 7. Diblock copolypeptides were synthesized by merely adding the correct molar amount of the second NCA to the polymer solution after the first block was synthesized. Most block copolypeptides were deprotected by trifluoroacetic acid and equimolar amounts of 33% HBr in acetic acid at 0°C for 1 hr. The deprotections of the block copolymers were usually accomplished under nitrogen in order to prevent hydrolysis of the peptide backbone. The exception to this was poly(L-cysteine<sub>30</sub>-*b*-L-lysine<sub>200</sub>) which was sometimes deprotected in air. If the poly(L-cysteine<sub>30</sub>-*b*-L-lysine<sub>200</sub>) was deprotected under nitrogen, the sulfhydryl residues remained in their reduced, thiol form whereas if the deprotection was done in air, disulfide bonds formed between the polymer chains. When samples of the oxidized poly(L-cysteine<sub>30</sub>-*b*-L-lysine<sub>200</sub>) were solubilized in water, a thick, viscous solution formed in contrast to that of the free-flowing solution which formed upon dissolving the reduced form of the polypeptide in water. The Ellman's reagent, 5-5'-Dithio-bis(2-nitrobenzoic acid), was used to determine the percentage of the disulfides formed when poly(L-cysteine<sub>30</sub>-*b*-L-lysine<sub>200</sub>) was deprotected in air. Using β-mercaptoethanol for the standard curve, it was calculated that approximately 70% of the cysteines were oxidized.

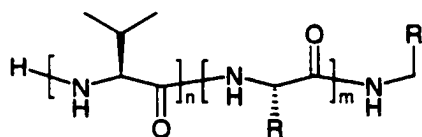
Some of the final block copolypeptides produced for biomimetic silica synthesis are shown below in Figure 39.



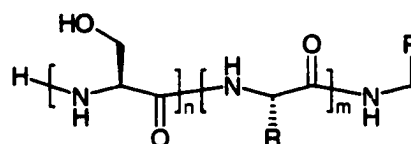
poly(L-alanine<sub>30</sub>-*b*-L-lysine<sub>200</sub>)



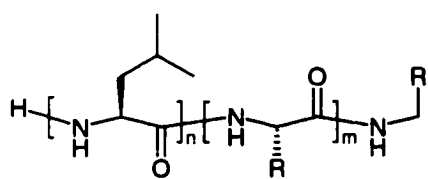
poly(L-cysteine<sub>30</sub>-*b*-L-lysine<sub>200</sub>)



poly(L-valine<sub>30</sub>-*b*-L-lysine<sub>200</sub>)

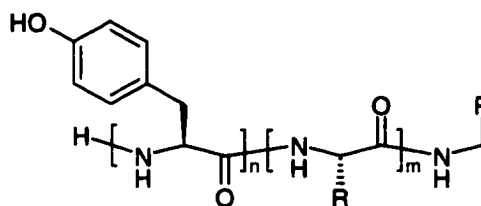


poly(L-serine<sub>30</sub>-*b*-L-lysine<sub>200</sub>)



poly(L-leucine<sub>30</sub>-*b*-L-lysine<sub>200</sub>)

**COLUMN A**

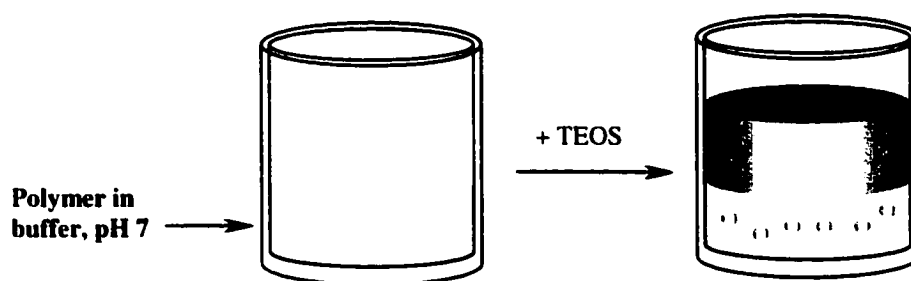


poly(L-tyrosine<sub>30</sub>-*b*-L-lysine<sub>200</sub>)

**COLUMN B**

**Figure 39.** A collection of the block copolypeptides that were synthesized as templates for biomimetic silica synthesis.

500  $\mu$ l of the diblock copolypeptides (5 mg/ml, 50mM Tris-HCl, pH 7) was mixed vigorously with 1.5 ml TEOS until the TEOS had emulsified into the aqueous phase as shown below. The reaction was then allowed to remain standing for 8 hours upon which any precipitate was collected, quantified as before and visualized by both light microscopy and SEM.



The reason why emulsion systems were used to create the silica structures was based on experience. Initially, another method of synthesis tried was to stir the TEOS and water layers for 6 to 10 hours at pH 7 and room temperature. Of the two synthesis preps tried, using an emulsion phase seemed to create the best ordered silica structures as viewed by microscopic studies. A possible explanation of how this occurs will be discussed later.

The quantity of silica that was produced using the various polypeptides was analyzed first. These numerical assays were done to see if certain amino acids could in fact hydrolyze silicon alkoxides such as TEOS at pH 7 as had been hypothesized. As before, any silica that was produced was first collected by centrifugation and washed several times with 95% ethanol to remove any unreacted TEOS. The silica was then hydrolyzed in NaOH at 95°C to  $\text{Si}(\text{OH})_4$  before quantification using the silicon molybdate assay. The amount of silica produced from using the various polypeptides are shown below in Table 8.

Block copolymer	SiO <sub>2</sub> Rate (μg/hr)	
	N <sub>2</sub>	Air
1. poly(L-alanine <sub>30</sub> - <i>b</i> -L-lysine <sub>200</sub> )	0.09 ± 0.002	
2. poly(L-valine <sub>30</sub> - <i>b</i> -L-lysine <sub>200</sub> )	0.03 ± 0.005	
3. poly(L-leucine <sub>30</sub> - <i>b</i> -L-lysine <sub>200</sub> )	0.09 ± 0.005	
4. poly(L-serine <sub>30</sub> - <i>b</i> -L-lysine <sub>200</sub> )	0.29 ± 0.003	
5. poly(L-tyrosine <sub>30</sub> - <i>b</i> -L-lysine <sub>200</sub> )	0.30 ± 0.007	
6. poly(L-cysteine <sub>30</sub> - <i>b</i> -L-lysine <sub>200</sub> )	0.43 ± 0.002	0.62 ± 0.004
7. poly(L-lysine <sub>200</sub> )	0.01 ± 0.001	
8. none	0.01 ± 0.001	

**Table 8.** The quantity of silica that was produced at pH 7 from reacting TEOS with the block copolypeptides

As shown in Table 8, the block copolypeptides from Column B in Figure 38 substantially produced a greater amount of silica as compared to those from Column A and presumably this is because of the nucleophilic nature of those block copolypeptides. It is also interesting to note that the amount of silica synthesized correlated to the nucleophilicity of the amino acids: poly(L-serine<sub>30</sub>-*b*-L-lysine<sub>200</sub>), poly(L-tyrosine<sub>30</sub>-*b*-L-lysine<sub>200</sub>) and poly(L-cysteine<sub>30</sub>-*b*-L-lysine<sub>200</sub>) respectively produced increasing amounts of silica. It is not understood as to why the oxidized poly(L-cysteine<sub>30</sub>-*b*-L-lysine<sub>200</sub>) produced more silica than its reduced form and it seems almost counterintuitive since the number of free nucleophilic sulfhydryl

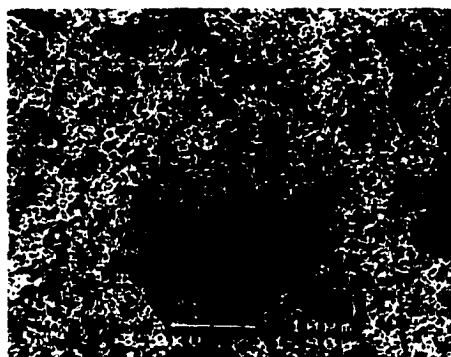
groups are lowered in the oxidized polypeptide.

It must be also noted though that poly(L-alanine<sub>30</sub>-L-lysine<sub>200</sub>) produced more silica than poly(L-lysine<sub>200</sub>) alone. One hypothesis is that this is because the hydrophobic blocks of the polymer draws or encapsulates more of the silicon alkoxide in the TEOS in water emulsion.

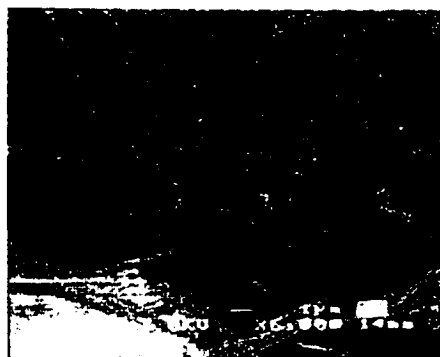
As stated in the beginning of Chapter 4, by incorporating nucleophilic amino acids in the organic template, ordered silica structures might be created since hydrolysis and subsequent condensation of the silicon alkoxide would occur directly at the organic inorganic interface. To test this hypothesis, samples of the silica produced were looked at by both light and scanning electron microscopy.

Although small amounts of silica were synthesized from using the block copolypeptides with the hydrophobic domains (polymers 1-3, Table 4), the reactions with these polymers were continued for 24-36 hours longer in order to see if the organic templates induced any morphological constraints on the silica produced. The silica precipitates that formed after a total of 44 hours were then compared to that of the silica produced after 8 hrs from the block copolypeptides 4-6 in Table 4. All of the samples were air-dried and sputter-coated with gold prior to being looked at under the SEM.

Figure 40 demonstrates a comparison of the silica formed from poly(L-alanine<sub>30</sub>-*b*-L-lysine<sub>200</sub>) and that from poly(L-serine<sub>30</sub>-*b*-L-lysine<sub>200</sub>), poly(L-tyrosine<sub>30</sub>-*b*-L-lysine<sub>200</sub>) and poly(L-cysteine<sub>30</sub>-*b*-L-lysine<sub>200</sub>) {AIR}.



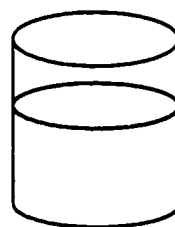
Silica produced from poly(L-alanine<sub>30</sub>-L-lysine<sub>200</sub>) after 44 hours



Silica produced from oxidized poly(L-cysteine<sub>30</sub>-L-lysine<sub>200</sub>) after 8 hours



Silica produced from poly(L-serine<sub>30</sub>-L-lysine<sub>200</sub>) after 8 hours



Silica produced from poly(L-tyrosine<sub>30</sub>-L-lysine<sub>200</sub>) after 8 hours

**Figure 40.** Scanning electron micrographs of the silica produced from reacting various block copolypeptides with TEOS at pH 7 and room temperature.

From the figures shown above, it is clearly discernible that using block copolypeptides with nucleophilic domains not only allow for the synthesis of silica at pH 7 but also produce structures with ordered morphologies. The silica formed after 44 hours of reaction from TEOS and poly(L-alanine<sub>30</sub>-*b*-L-lysine<sub>200</sub>) is a completely amorphous, disordered precipitate which is not unlike that which is formed from adding nanopure water alone to TEOS at pH 7 for 2-3 days. On the other hand, poly(L-serine<sub>30</sub>-*b*-L-lysine<sub>200</sub>) produced "spheres", poly(L-tyrosine<sub>30</sub>-*b*-L-lysine<sub>200</sub>) produced a semi-transparent gel and oxidized poly(L-cysteine<sub>30</sub>-*b*-L-lysine<sub>200</sub>) produced lathelike bundles of silica--all within 8 hours. These results demonstrate that building in catalytic functional groups at the organic inorganic interface allows one to synthesize silica at physiological pHs and temperature from TEOS and that the organization of the organic groups ultimately plays a hand at governing the final morphology of the silica structures. Although this was not studied in any detail, the overall rate at which the silicon alkoxide is hydrolyzed may also play a distinct role in controlling the silica polymerization.

One key experiment that was done to analyze the influence of the self-assembled organic template on silica shape was to compare the silica synthesized from both the reduced and oxidized forms of poly(L-cysteine<sub>30</sub>-L-lysine<sub>200</sub>). When the block copolypeptide was deprotected under nitrogen, all of the cysteines would remain as free sulhydryl groups and the polymer should self-assemble quite differently from that of its oxidized form where disulfide bridges would exist



between the polymer chains. After deprotecting the polypeptide under a continuous source nitrogen, it was handled exclusively in a glove box to prevent any oxidation of the sulfhydryl groups. The silica synthesis was done as previously mentioned and the quantity of silica produced is shown in Table 8. But the more important and the more dramatic result is shown in Figure 41.

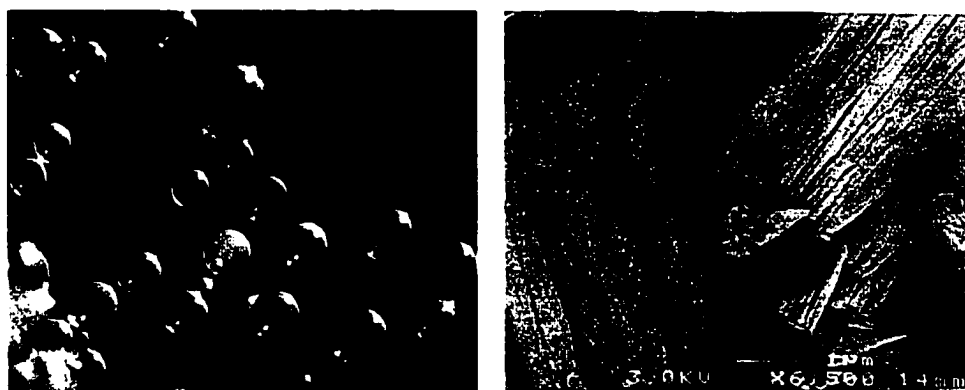
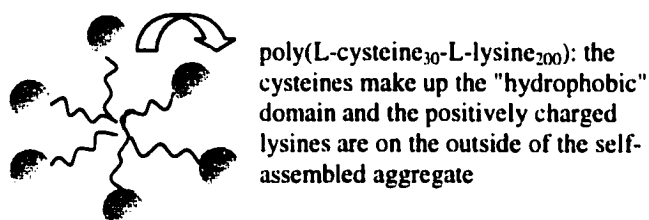


**Figure 41.** Light and scanning electron micrograph images of the different silica structures produced from poly(L-cysteine<sub>30</sub>-L-lysine<sub>200</sub>) and TEOS at pH 7. In the left panel, 100 $\mu$ m, hard, transparent spheres were synthesized when using the poly(L-cysteine<sub>30</sub>-L-lysine<sub>200</sub>) which had been deprotected under nitrogen. In the right panel, lathlike bundles of silica were produced when using the polypeptide which had been deprotected in air.

In order to achieve a better understanding of the process in which the block copolypeptides create such ordered silica structures, a detailed study of the polypeptide's interaction with the silica moieties needs to be done. Currently, we are working toward being able to do some <sup>29</sup>Si MAS NMR studies. Because <sup>13</sup>C

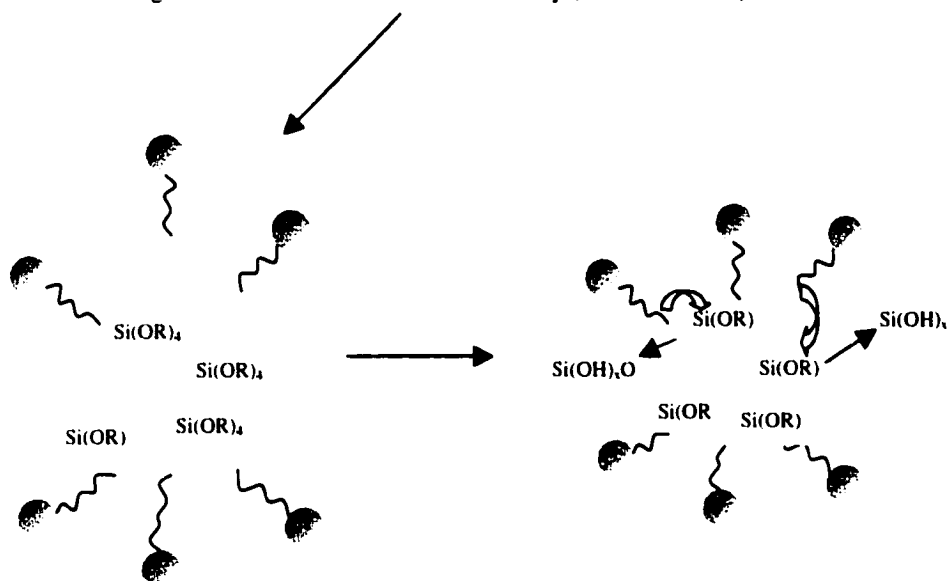
and  $^{15}\text{N}$  labeled amino acids are so expensive (approximately \$250 for 0.5 grams), a substantial amount of effort has gone into figuring out the most efficient way to put protecting groups on the natural amino acids for NCA synthesis.

Nevertheless, even without the NMR analyses, a hypothetical scheme can be introduced.



Schematic diagram of the self-assembly of the reduced form of poly(L-cysteine<sub>30</sub>-L-lysine<sub>200</sub>)

After adding TEOS → emulsion chemistry (TEOS in water)

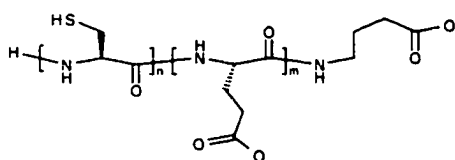


The cysteines of the diblock copolyptide hydrolyze the TEOS molecules to  $\text{Si}(\text{OH})_x\text{O}^-$ , and these charged silica molecules diffuse to the aqueous layer and migrate by charge attraction to the positively charged poly-L-lysine block. Polycondensation to  $\text{SiO}_2$  will occur at the polycationic surface.

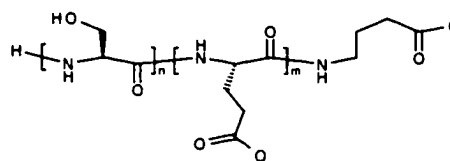
**Figure 42.** A hypothetical scheme how silica synthesis occurs in the emulsified TEOS and block copolyptide system.

Through either disulfide bonds or hydrogen bonding, the cysteine residues of the block copolypeptide, poly(L-cysteine<sub>30</sub>-L-lysine<sub>200</sub>) aid in the self-assembly of the polymer chains. The cysteine's interaction with each other should cause a "hydrophobic" domain to form in the self-assembled polymer matrix. When a silicon alkoxide such as TEOS is added to the polypeptide solution, it will therefore be drawn to this "hydrophobic" pocket. Hydrolysis of the alkoxide will occur by the cysteines and the now hydrophilic and negatively charged silicic acid species will migrate to the positively charged lysine amino acids of the block copolypeptide, where they will undergo condensation to silica. This hypothetical scheme will be tested for using isotopically labeled block copolypeptides and both solution and solid state NMR analysis.

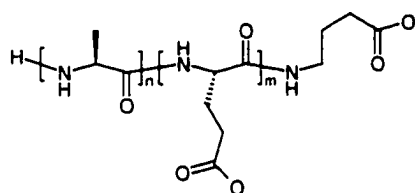
In order to test the importance of the positively charged lysine domain, negatively charged L-glutamic acid was used instead and the synthesized polymers are shown below.



poly(L-cysteine<sub>30</sub>-L-glutamate<sub>200</sub>)



poly(L-serine<sub>30</sub>- glutamate<sub>200</sub>)



poly(L-alanine<sub>30</sub>-L-glutamate<sub>200</sub>)

The glutamic acid incorporated block copolypeptides were synthesized using BipyNiCOD as the initiator and the reactions were done in DMF. The deprotection of the polymers were either done under a constant flow of nitrogen using either trimethylsilyliodide (TMS Iodide) or 33% HBr in acetic acid. Following the deprotection, the block copolypeptides initially had to be solubilized in water using molar equivalents of NaOH and this was then followed by extensive dialysis against nanopure water.

When any of the glutamic acid block copolypeptides mentioned were reacted with TEOS at pH 7, surprisingly, little or no silica was produced. This is especially puzzling since previously, poly-L-cysteine alone acted as a sufficient enough catalyst for TEOS hydrolysis at neutral pH. While this supports the hypothesis that polycations are important for interacting with negatively charged silicate precursors, the complete inhibition of the nucleophilic domains to catalyze the TEOS reaction remains unexplained. One hypothesis is that it may be that the polyanionic polymers help stabilize the negatively charged silica species and prevent polycondensation to silica.

- (1) Israelachvili, J.N. *Intermolecular and Surface Forces*, 2<sup>nd</sup> Ed., Academic Press, London (1992)
  
- (2) Woodward, J., Tate, J., Hermann, P.C., Evans, B.R. *Jou. Biochem. Biophys. Methods*, **26**, 121-129 (1993)
  
- (3) Strickland, J.D.H. & Parsons, T.R. *A Practical Handbook of Seawater Analysis* (Fisheries Research Board of Canada, Ottawa), 2<sup>nd</sup> Ed. (1972)
  
- (4) Cha, J.N., Stucky, G.D., Morse, D.E., Deming, T.J. *Nature*, **403**, 289-292 (2000)